Characterization of Chloroplast Protein Import without Tic56, a Component of the 1-Megadalton Translocon at the Inner Envelope Membrane of Chloroplasts[1]

Daniel Köhler, Cyril Montandon, Gerd Hause, Petra Majovsky, Felix Kessler, Sacha Baginsky, and Birgit Agne*

Institut für Biochemie und Biotechnologie (D.K., S.B., B.A.) and Biozentrum (G.H.), Martin-Luther-Universität Halle-Wittenberg, 06120 Halle (Saale), Germany; Laboratory of Plant Physiology, University of Neuchâtel, 2000 Neuchatel, Switzerland (C.M., F.K.); and Research Group Proteome Analytics, Leibniz Institute of Plant Biochemistry, 06120 Halle (Saale), Germany (P.M.)

We report on the characterization of Tic56, a unique component of the recently identified 1-MD translocon at the inner envelope membrane of chloroplasts (TIC) in Arabidopsis (*Arabidopsis thaliana*) comprising Tic20, Tic100, and Tic214. We isolated Tic56 by copurification with Tandem Affinity Purification-tagged Toc159 in the absence of precursor protein, indicating spontaneous and translocation-independent formation of the translocon at the outer envelope membrane of chloroplasts (TOC) and TIC supercomplexes. Tic56 mutant plants have an albino phenotype and are unable to grow without an external carbon source. Using specific enrichment of protein amino termini, we analyzed the *tic56-1* and *plastid protein import2* (*toc159*) mutants to assess the in vivo import capacity of plastids in mutants of an outer and inner envelope component of the anticipated TOC-TIC supercomplex. In both mutants, we observed processing of several import substrates belonging to various pathways. Our results suggest that despite the severe developmental defects, protein import into Tic56-deficient plastids is functional to a considerable degree, indicating the existence of alternative translocases at the inner envelope membrane.

Chloroplast functions depend on the import of several thousand nucleus-encoded proteins that enter the chloroplast through different import pathways (for review, see Jarvis, 2008; Shi and Theg, 2013). The prevalent pathway for most of the proteins with photosynthetic and housekeeping functions operates via complexes in the outer and inner envelope membranes of chloroplasts, designated as TOC and TIC translocon complexes (Schnell et al., 1997). The majority of nucleus-encoded plastid proteins that enter chloroplasts through the TOC/TIC system possess a cleavable N-terminal transit peptide that mediates their specific import into different plastid types. Previous reports suggested that plastid transit peptides contain functional motifs that determine their preference for different plastid types (von Heijne et al., 1989; Pilon et al., 1995; Ivey et al., 2000; Chotewutmontri et al., 2012; Teng et al., 2012; Li and Teng, 2013). These analyses clearly support the view of import specificity that depends on the developmental status of the chloroplast. It is conceivable that this selectivity is mediated through the initial recognition of precursor proteins at the chloroplast surface (i.e. that the selectivity is mediated by different receptor protein complexes at the outer envelope membrane).

Indeed, plastids possess structurally and functionally distinct TOC complexes that differentiate between different client proteins and establish precursor protein selectivity (Jarvis et al., 1998; Bauer et al., 2000; Kubis et al., 2003, 2004; Ivanova et al., 2004). In green Arabidopsis (*Arabidopsis thaliana*) tissues, the predominant TOC core complex is built from the receptor GTPases Toc159 and Toc33 and the translocation channel Toc75. In alternative TOC complexes, the two GTPases are replaced by their homologs, whereby their substrate selectivity is largely determined by the different receptors of the Toc159 family (Smith et al., 2004; Inoue et al., 2010). The current model suggests that TOC complexes built around Toc159 and Toc90 are mainly involved in the import of photosynthetic proteins (Bauer et al., 2000; Infanger et al., 2011), while the Toc132- and Toc120-containing complexes mediate the import of housekeeping proteins (Ivanova et al., 2004; Kubis et al., 2004). This model explains the ability of chloroplasts to import low-abundance proteins under conditions of high photosynthetic protein import. Proteomic analyses challenged this model because many photosynthetic proteins were found imported in *plastid protein import2* (*ppi2*) plastids lacking Toc159, and the decreased accumulation of photosynthetic complexes is largely explained by their down-regulation at the transcriptional level (Bischof et al., 2011). A recent large-scale split-ubiquitin study suggested overlapping precursor-binding specificities of Toc159 and Toc132, which could

[1]This work was supported by the Deutsche Forschungsgemeinschaft (grant no. Ba1902/3–1 to S.B.).

* Address correspondence to birgit.agne@biochemtech.uni-halle.de.

The author responsible for distribution of materials integral to the findings presented in this article in accordance with policy described in the Instructions for Authors (www.plantphysiol.org) is: Birgit Agne (birgit.agne@biochemtech.uni-halle.de).

www.plantphysiol.org/cgi/doi/10.1104/pp.114.255562

explain the occurrence of a subset of photosynthetic proteins in the *ppi2* chloroplast proteome (Dutta et al., 2014). Thus, the mechanisms mediating the selective import of preproteins into plastids remain elusive.

Different members of the Toc159 family of receptor proteins differ in the length of a conserved acidic domain, the so-called A domain (Hiltbrunner et al., 2001a). Two studies suggest that the A domains confer specificity to the different members of the Toc159 family (Inoue et al., 2010; Dutta et al., 2014). This could explain why full-length Toc120 or Toc132 fails to complement the *ppi2* mutant (Kubis et al., 2004), while a construct of Toc132 lacking the A domain was partially able to do so (Inoue et al., 2010). These data suggest that fully assembled TOC complexes with different members of the Toc159 family must be present in the outer envelope membrane to support specific protein import during chloroplast development, which is in line with a reorganization of the import machinery in phases of changing protein import demand. Indeed, Ling et al. (2012) identified a REALLY INTERESTING NEW GENE ubiquitin ligase as a suppressor of the pale-green phenotype of a Toc33 mutant (*ppi1*) and showed that the ubiquitin proteasome system controls the assembly of different TOC complexes by regulated proteolysis. As anticipated, this reorganization is especially relevant during etioplast-to-chloroplast and chloroplast-to-gerontoplast differentiation. In the case of etioplast-to-chloroplast conversion, the increasing demand for the import of photosynthetic proteins is apparently accompanied by the disassembly of TOC complexes that have different specificities. However, evidence for the preferential degradation of Toc132 and/or Toc120 during plastid differentiation by the ubiquitin proteasome system is currently missing.

It is currently unclear how far the association of TOC complexes with different TIC components contributes to precursor selectivity. Thus, a full understanding of client protein specificity requires the analysis and identification of translocation-competent TOC-TIC supercomplexes. In contrast to the TOC translocon, the organization and subunit composition of the TIC complexes are less clear and under controversial debate. For Tic20 and Tic110, translocon channel activity has been demonstrated in vitro (Heins et al., 2002; Balsera et al., 2009; Kovács-Bogdan et al., 2011; Kikuchi et al., 2013). However, it is still in question if these proteins are part of two functionally distinct import routes. Recently, a new 1-MD TIC complex was identified that was termed the general import translocon. This complex is built around Arabidopsis Tic20-I and comprises Tic56, Tic100, and the chloroplast-encoded hypothetical chloroplast open reading frame 1.2 gene product termed Tic214 (Kikuchi et al., 2013). Tic110 and Tic40 were absent from this complex, arguing for a separate function of the Tic110 complex. Lack of Tic56 and Tic100 resulted in strongly reduced levels of the 1-MD TIC translocon and in albino phenotypes resembling the phenotype of the *tic20-I* mutant, further supporting a common function in the 1-MD complex. However, the import capacity of the *tic56* and *tic100* albino mutants has not been directly tested yet.

Characterization of a system as complex as plastid protein import requires specialized tools that allow an unbiased identification of client proteins for the different receptors. Functional proteomics allows an assessment of protein accumulation in the absence of specific receptors or import components. While a standard proteomics experiment is useful and provides information on plastid protein accumulation, protein N termini are of specific interest because they allow distinguishing imported and correctly processed proteins from accumulated precursors (Bischof et al., 2011). One out of several methods for the analysis of protein N termini is called terminal amine isotopic labeling of substrates (TAILS; Kleifeld et al., 2010; Lange and Overall, 2013). In TAILS, protein N termini are blocked by dimethyl labeling, and newly generated N termini from the subsequent tryptic digestion are removed by their coupling to a polymer. This subtractive approach has been employed successfully for the characterization of protein processing and transport into plastids of the diatom *Thalassiosira pseudonana* (Huesgen et al., 2013). Here, we used the TAILS method in combination with protoplast import assays and in vitro import kinetics to characterize the contribution of Tic56 and the 1-MD TIC complex to plastid protein import and compare these data with those from the *ppi2* mutant deficient in Toc159 (Bauer et al., 2000). Our data reveal a considerable degree of protein import into both mutants and allow pinpointing Toc159- and Tic56-independent client proteins.

RESULTS

Coisolation of Tic56 with Affinity-Tagged Toc159

In a precedent study, we used transgenic Arabidopsis plants expressing the Protein A-tagged chloroplast protein import receptor Toc159 to isolate Toc159 from a solubilized whole-cell membrane fraction (Agne et al., 2010). Pursuing this approach to identify new components of the chloroplast protein import machinery, the purification experiment was scaled up and the eluates (Fig. 1A) were subjected to mass spectrometric analysis. Mass spectrometry (data not shown) revealed that Tic56, a component of the recently uncovered 1-MD TIC complex (Kikuchi et al., 2013), specifically copurified with Toc159.

An antiserum was raised against recombinant Tic56. The Tic56-specific antiserum detects a protein at approximately 63 kD by SDS-PAGE that is not detected in protein extracts of the Arabidopsis transfer DNA (T-DNA) insertion mutants *tic56-1* and *tic56-3* (Fig. 1B), supporting the specificity of this antibody preparation. Tic56 migrates at a higher molecular mass than predicted (56.3 kD), which is probably due to the high content of acidic residues, particularly in its C-terminal part. In *tic56-1*, which is a null mutant of *TIC56* (Kikuchi et al., 2013), only one 70-kD cross-reactive band was detected, whereas in the *tic56-3* mutant, additional bands at 130 kD and approximately 48 kD appeared (Fig. 1B, center). These signals are potentially Tic56 specific, as the mutant has the T-DNA insertion in the last exon of the *TIC56* gene (Kikuchi et al.,

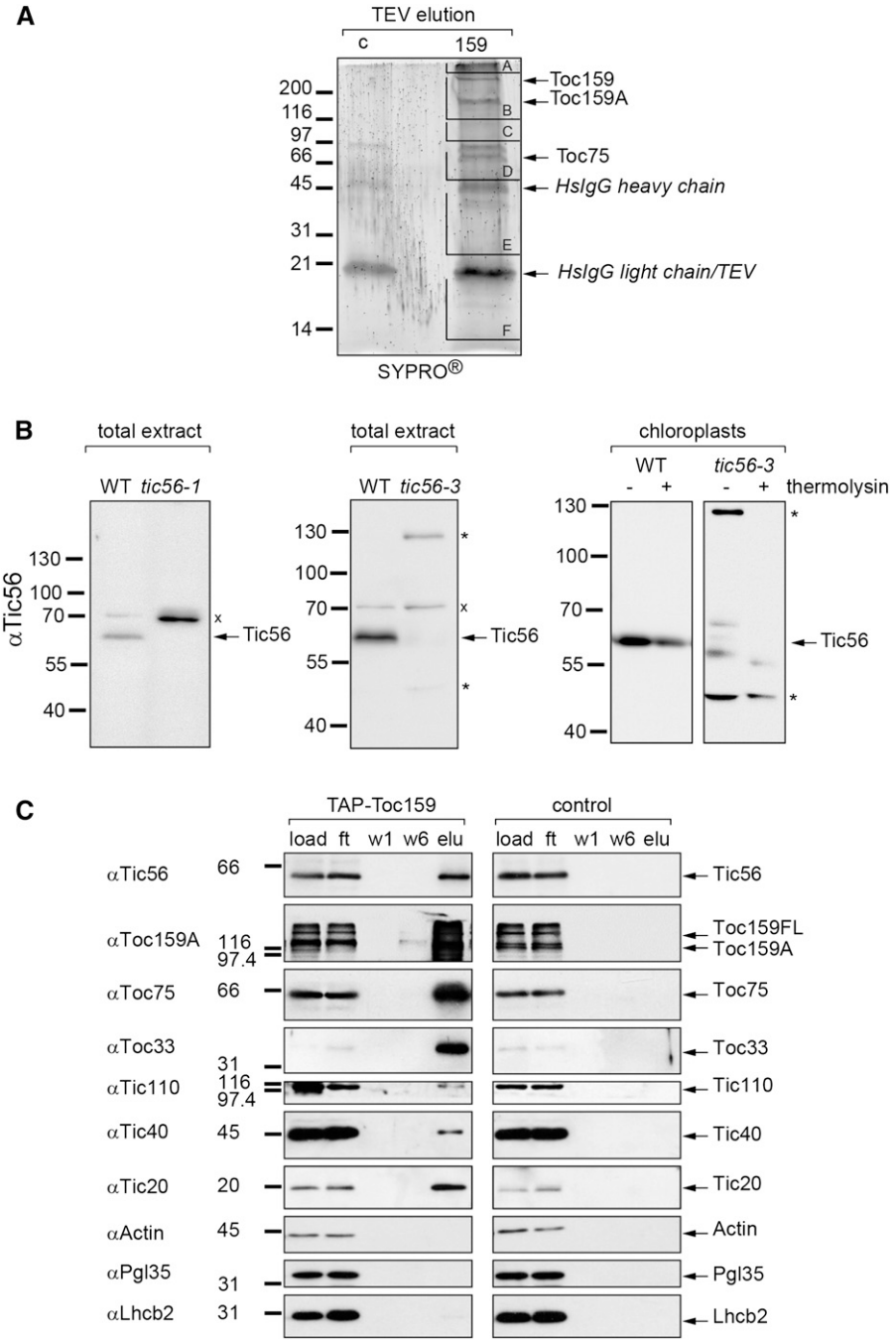

Figure 1. Association of Toc159 with Tic56, a component of the 1-MD TIC complex. A, SyproRuby stain of an eluate obtained after the purification of TAP-Toc159 from Triton X-100-solubilized membrane proteins of TAP-Toc159:*ppi2* plants (159). As a control, the same purification procedure was performed with wild-type plants (c). Subsequent mass spectrometric analysis of gel slices A to F revealed the presence of Tic56 peptides in gel slice D (data not shown). B, Specificity of the anti-Tic56 serum. Fifty micrograms of protein of total protein extracts of the wild type (WT) and of two *tic56* T-DNA insertion mutants (*tic56-1* on the left and *tic56-3* in the center) was analyzed by SDS-PAGE and immunoblotting with anti-Tic56 antiserum. Each x indicates a 70-kD cross reaction of the serum with a protein present in wild-type and mutant samples. To further analyze the additional bands (asterisks) appearing in *tic56-3*, chloroplasts of 16-d-old wild-type and *tic56-3* seedlings were isolated, treated or not with thermolysin (50 μg mL^{-1}), and subjected to the same immunoblotting procedure. C, Confirmation of the copurification of Tic56 with Toc159 by immunoblotting of fractions from a TAP-Toc159 purification. Fifty micrograms of protein of Triton X-100-solubilized membrane proteins loaded to *Homo sapiens* (Hs)IgG beads (load), 50 μg of the column flow through (ft), and 25% of two different wash fractions (w1 and w6) and the tobacco etch virus protease eluates (elu) were probed with antisera as indicated.

2013; Supplemental Fig. S1). Thus, in *tic56-3*, elongated or truncated forms of Tic56 can be expected depending on the translation of in-frame coding sequences residing on the T-DNA. Both the 130- and 48-kD proteins can be detected in isolated *tic56-3* chloroplasts, but only the 48-kD protein was resistant to thermolysin treatment of chloroplasts and behaved like wild-type Tic56 (Fig. 1B, right). Kikuchi et al. (2013) exclusively detected a truncated form of Tic56 in *tic56-3*. We assume that the 48-kD protein identified here corresponds to the truncated form described by Kikuchi et al. (2013). It remains undetermined if this truncated form results from a premature stop codon or if it is a stable degradation product of a higher molecular mass Tic56 fusion protein.

With the anti-Tic56 antiserum, we confirmed the interaction of Tic56 with Toc159 (Fig. 1C). Tic20, the channel protein and key component of the 1-MD TIC complex, also was found to be enriched in the eluates of the TAP-Toc159 purification experiment. In addition to Tic56 and Tic20, other members of the TOC core complex, Toc33 and Toc75, as well as Tic110 and Tic40, also were detected in the eluates by western blotting (Fig. 1C). Our data indicate that protein import supercomplexes between Toc159 and different TIC complexes

can be isolated in the absence of any externally added precursor protein. In the following, we report on the functional characterization of Tic56 in the context of chloroplast biogenesis and the import capacity of *TIC56*-deficient mutants.

Disturbed Plastid Development in *tic56-1* Plants

Lack of Toc159 as well as Tic56 results in seedling-lethal albino phenotypes in Arabidopsis (Bauer et al., 2000; Kikuchi et al., 2013; Supplemental Fig. S2). However, the two albino mutants *ppi2* (*toc159*) and *tic56-1* are phenotypically not identical. Compared with the Toc159-deficient mutant *ppi2*, *tic56-1* plants have a more severe phenotype with less residual chlorophyll and irregularly shaped, nearly translucent ivory-colored leaves (Fig. 2A; Supplemental Fig. S2). Cross sections of 8-week-old *tic56-1* leaves reveal a loss of cellular organization with reduced mesophyll and the absence of mature chloroplasts (Fig. 2A). In transmission electron micrographs, plastids of *tic56-1* appear to be two to three times smaller and variable in shape compared with their wild-type counterparts. Furthermore, *tic56-1* plastids lack a thylakoid network characteristic of mature chloroplasts (Fig. 2B). Only a few presumably (pro)thylakoid membranes that are associated with plastoglobules can be observed. These results confirm that Tic56 is required for chloroplast development.

Levels of Other TOC and TIC Components in *tic56-1*

The coisolation of Tic56 with the chloroplast import receptor Toc159 and its presence in the recently identified 1-MD TIC complex suggest that the *tic56-1* mutant has a defect in plastid protein import. In *tic56-1*, Tic56 is lacking and the other components of the 1-MD Tic20 complex (Tic20, Tic100, and Tic214) do not accumulate (Kikuchi et al., 2013). Therefore *tic56-1* is ideal for the characterization of plastid protein import in the absence of the 1-MD TIC complex that was designated as the general TIC translocon. Because Tic56 associates with a Toc159-containing complex (Fig. 1), we tested whether the absence of Tic56 perturbs the integrity of the TOC translocon by western blotting (Fig. 3). The TOC components Toc159, Toc132, and Toc75 as well as Tic110 and Tic40 were detected at normal or even higher levels in the mutant plants compared with the wild-type control. Higher TOC/TIC protein levels were detected also in other albino mutants with defects in genes unrelated to chloroplast protein translocation (Motohashi et al., 2012). Thus, our data suggest that a lack of Tic56 perturbs neither the TOC translocon nor the Tic110-Tic40 complex. Toc75 and Tic40 have transit peptides and are processed to their mature size in *tic56-1*, indicating that, despite the absence of the 1-MD TIC complex, a subset of proteins is still imported. On the contrary, nucleus-encoded light harvesting complex of PSII (Lhcb4) and the small subunit of Rubisco (SSu) as well as plastid-encoded PSII reaction center protein A (PsbA) were not detectable in the *tic56-1* total leaf extract,

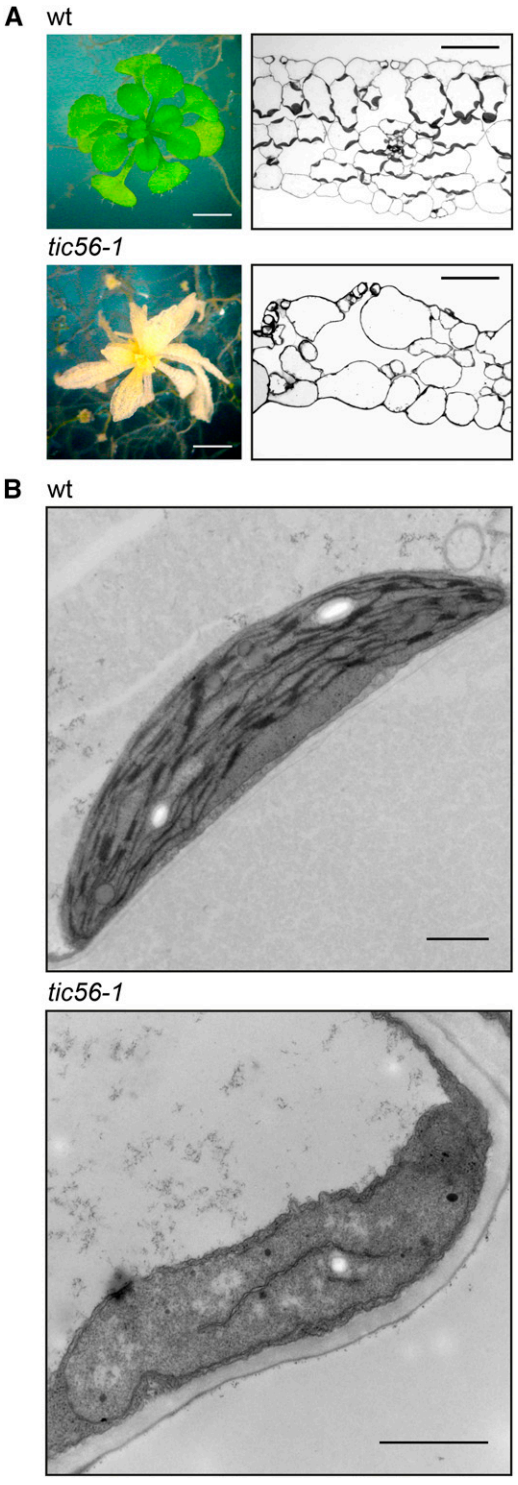

Figure 2. Disturbed leaf morphology and plastid development in *tic56-1* plants. A, Leaf cross sections of 8-week-old wild-type (wt) and *tic56-1* plants show disordered tissue and lack of chloroplasts of *tic56-1* leaves. Bars = 2 mm (plant images) and 50 μm (cross sections). B, Transmission electron micrographs of wild-type and *tic56-1* plastids uncover differences in the overall structure, in the shape and size of the organelles as well as in their stroma-localized membrane system. Bars = 1 μm.

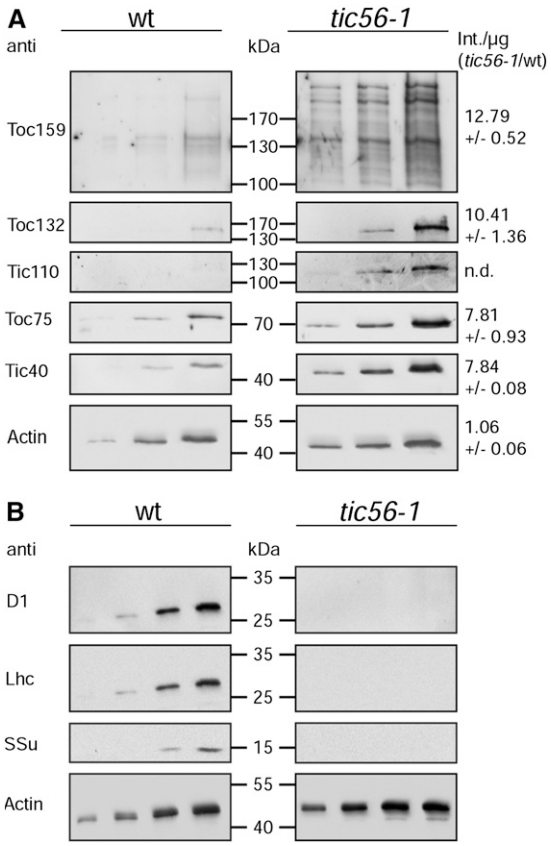

Figure 3. Western-blot analysis of TOC components, Tic110/Tic40 (A) and different plastid proteins involved in photosynthesis (B), in *tic56-1* compared with the wild type. Rising protein amounts (top, 10, 20, and 50 μg; bottom, 2, 4, 8, and 12 μg) of 8-week-old wild-type (wt) and *tic56-1* leaves were loaded and analyzed with antibodies as indicated. Detection of actin served as a loading control. In A, the ratio between the signal intensities (Int.) per μg of protein of *tic56-1* and the wild type is given alongside the blots.

suggesting either substrate specificity in the disturbed import process or a systemic regulation at the level of transcription (Richly et al., 2003).

Analysis of Protein Import into *tic56-1* Plastids by N-Terminal Peptide Identification

We decided to investigate the import ability and selectivity of *tic56-1* mutant plastids by an unbiased experimental approach that provides direct evidence for functional import and is not restricted to a few selected import substrates. The method we have chosen is TAILS, which is based on the specific identification of N-terminal peptides by mass spectrometry. Protein extracts of the wild type, *tic56-1*, and *ppi2* were denatured, and the naturally occurring free N termini of proteins were blocked by dimethylation followed by tryptic digestion. The internal peptides generated by trypsin were subsequently removed by their coupling to a high-molecular-weight dendritic hyperbranched polyglycerol-aldehyde polymer and subsequent filtration. The resulting flow through that is enriched for in vivo N termini was analyzed by liquid chromatography-tandem mass spectrometry on an Orbitrap Velos device (Thermo Scientific). In total, N-terminal peptides of 348 proteins were identified from wild-type, 280 from *ppi2*, and 481 from *tic56-1* plant material (Supplemental Table S1).

Figure 4A (top) shows the relative distribution of the minimal N-terminal peptide of the identified proteins in relation to their corresponding full-length sequences. The proteins were sorted according to the positions of the start amino acids of their most N-terminal peptides. The amount of proteins falling into a starting range is given in percentage of total proteins identified. The pattern of minimal peptide distribution was nearly identical for the three different plant lines, with local maxima at the amino acid position 1 or 2, 21 to 30, and 51 to 60 and at positions greater than 150. Proteins in the 1 or 2 starting bin comprise mostly cytosolic proteins or proteins encoded by organellar genomes. The local maximum at bin 21 to 30 is based on mostly nucleus-encoded processed mitochondrial proteins that generally have shorter N-terminal targeting sequences than plastid proteins (Supplemental Table S2; Huang et al., 2013). Accordingly, these two maxima remain when only nonplastid proteins are plotted in the histogram (Fig. 4A, middle). A closer look at the starting positions of plastid proteins shows that the 21 to 30 bin also comprises several processed plastid proteins. However, most plastid proteins started with amino acids 51 to 60 (Fig. 4A, bottom). The accumulation of proteins with starting positions greater than 150 can be explained by additional proteolytic processing that affects the in vivo accumulation of protein N termini mainly of nonplastid proteins.

As the bulk of chloroplast proteins in all lines started in the range of amino acids 21 to 90 (Fig. 4A, bottom), these data clearly show that many chloroplast proteins are imported into the plastids of both mutants lines and that these are processed to a mature or nearly mature form by transit peptide removal after import. Only a few plastid proteins started with the first or second amino acid, and these are almost exclusively plastid-encoded proteins (Fig. 4A, bottom). Exceptions are two proteins in *tic56-1* as well as four proteins in *ppi2* that were found as unprocessed precursor proteins (Table I).

The Venn diagram in Figure 4B gives an overview of the overlap of nucleus-encoded plastid proteins identified in the three different plant lines.

Comparison of Experimental and Predicted N Termini of Imported Plastid Proteins

To validate the correct processing of the imported substrates, their transit peptide length was predicted using ChloroP (Emanuelsson et al., 1999) and the predicted and measured transit peptide lengths were compared (Fig. 4C). As shown in Figure 4C, the measured starting positions for most of the nucleus-encoded plastid proteins in the wild type, *ppi2*, and *tic56-1* matched the prediction by ChloroP perfectly (Δ0) or was shifted by one toward the

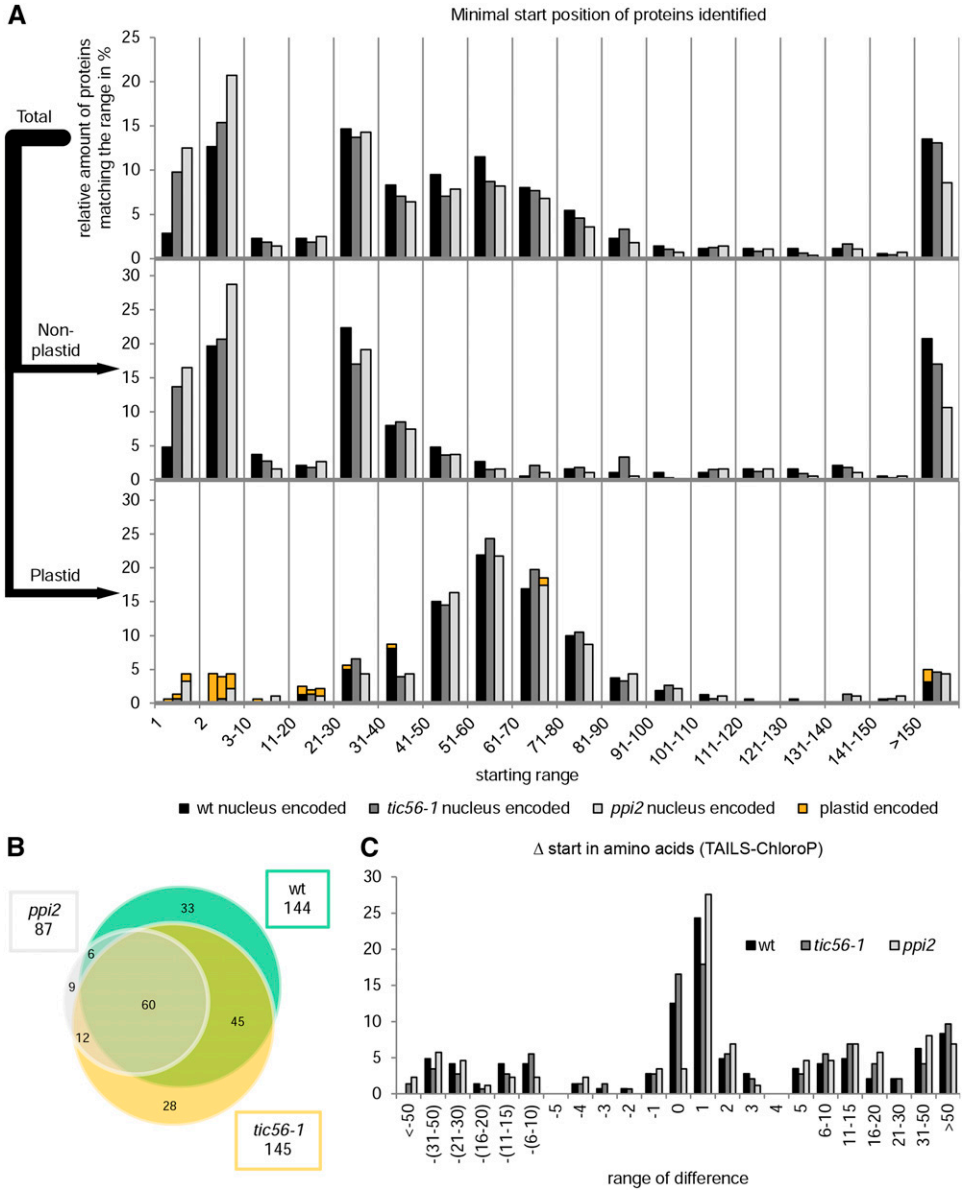

Figure 4. TAILS analyses of *tic56-1*, *ppi2*, and the wild type. A, Distribution of the minimal starting positions in the annotated full-length sequences of proteins identified by TAILS. For each identified protein, the most N-terminal peptide identified by the TAILS experiment was determined and grouped into starting ranges as indicated. The amount of proteins falling into a distinct range was set into relation with the total number of proteins of each plant line. In the graph at top, the minimal starting positions of all proteins identified are shown. The middle and bottom graphs show the distribution of starting positions of nonplastid or plastid proteins, respectively. The key at the bottom includes additional information about where the proteins are encoded (nucleus, black, dark gray, and light gray; plastid, orange). The first bar in each group always represents the wild type (wt), the second bar always represents *tic56-1*, and the third bar always represents *ppi2*. Chloroplast proteins were classified according to a chloroplast reference proteome (van Wijk and Baginsky, 2011). B, Venn diagram of nucleus-encoded plastid proteins identified for *tic56-1*, *ppi2*, and the wild type. C, The difference between the experimental (TAILS) and predicted (ChloroP) starting positions of the proteins was calculated. Positive values signify processing downstream, and negative values signify processing upstream of the theoretical processing site.

subsequent amino acid (Δ1). Remarkably, this shift in the starting positions of plastid proteins was much more pronounced in the *ppi2* mutant than in the wild type and *tic56-1*. The observed discrepancy between the ChloroP-predicted and experimental starting amino acids is striking but has been observed in previous studies dealing with the N termini of the plastid proteins (Emanuelsson et al., 1999; Zybailov et al., 2008; Huesgen et al., 2013). A statistical evaluation of the processing site by sequence logo revealed that Cys and Ala are frequently removed compared with

Table I. *Identified unprocessed precursor proteins in the mutant lines tic56-1 and ppi2*

Line	Identifier	Description	Start Position	N-Terminal Peptide	Natural Modification
tic56-1	AT4G34200.1	EDA9 (EMBRYO SAC DEVELOPMENT ARREST9)	2	SATAAASSSIAVATNSLR	*N*-Acetyl
	AT5G56730.1	Peptidase M16 family	1	MDLIAGESSkVLR	*N*-Acetyl
ppi2	AT1G60950.1	FED A (FERREDOXIN2)	2	ASTALSSAIVGTSFIR	*N*-Acetyl
	AT2G33800.1	Ribosomal protein S5 family protein	2	ATASALSSLSSLSLHTR	*N*-Acetyl
	AT4G17090.1	CT-BMY (β-AMYLASE3, β-AMYLASE8)	1	MELTLNSSSSLIkR	*N*-Acetyl
	AT5G56730.1	Peptidase M16 family	1	MDLIAGESSkVLR	*N*-Acetyl

the prediction (Supplemental Fig. S3A, bottom, position −1), thus changing the starting amino acids of the affected proteins. Indeed, we observed that among the experimentally determined N termini, Ala occurred much less frequently than predicted (Supplemental Fig. S3B). Furthermore, no protein was found with an N-terminal Cys. In contrast, Ser occurred significantly more often in the experimental data set compared with the prediction (Supplemental Fig. S3B), suggesting a regulatory mechanism to control the N-terminal amino acid in vivo.

Tables II to V present the proteins that are correctly imported and processed in the two albino mutants *ppi2* and *tic56-1*. From these data, we inferred import to the thylakoid lumen. We observed thylakoid proteins with removed bipartite targeting signals, suggesting that both import mutants have functional translocation machineries to transport proteins into the thylakoid lumen. This holds true for substrates of both the secretory (Sec) and the twin arginine translocase (Tat) pathways (Tables II and IV).

Several of the processed substrates were found in both mutants; however, for some of them, the starting amino acid turned out to be different in *ppi2* and *tic56-1* (Tables II–V). Indeed, whenever the starting amino acid of a protein in *ppi2* differed from *tic56-1* or the wild type, one or two amino acids were lacking (Tables II–V; Supplemental Table S1). This indicates that the potential regulatory mechanism controlling the N-terminal amino acid in vivo might function differently in the two import mutants.

Correct removal of the transit peptide is strong evidence for the import of a substrate into chloroplasts; however, it is possible that some precursor proteins become processed before they have completely passed across the envelope. To check if plastid proteins in *tic56-1* are exposed at the organellar surface, we treated a crude plastid preparation of the wild type and *tic56-1* with thermolysin, a protease not penetrating the outer envelope (Cline et al., 1984). Subsequently, the proteome of thermolysin-treated plastids was analyzed by liquid chromatography-tandem mass spectrometry on an Orbitrap Velos device (Thermo Scientific). Here, we found many peptides mapping to the C-terminal region of plastid proteins in the

Table II. *Correctly processed plastid proteins identified with TAILS in ppi2 (thylakoid proteins)*

Chloroplast proteins are listed that were identified in their mature (i.e. correctly processed) form on the basis of their N-terminal peptides in *ppi2*. Most processing events of nucleus-encoded plastid proteins are consistent with the ChloroP prediction or the UniProt entry for thylakoid lumenal proteins, arguing for functional import and functional processing peptidases. Thylakoid proteins were classified according to AT_CHLORO (Ferro et al., 2010). Proteins were classified into pathways using MapMan (Thimm et al., 2004).

Identifier	Description	Start, TAILS	Start, ChloroP/UniProt	MapMan Classification/Thylakoid Import Pathway
AT1G03600.1	PSB27/PSII family protein	69	68/69	PS.lightreaction.photosystem II.PSII polypeptide subunits/ Tat
AT1G31330.1	PSAF/PSI subunit F	68	33/68	PS.lightreaction.photosystem I.PSI polypeptide subunits/ not assigned
AT1G54780.1	TLP18.3/thylakoid lumen 18.3-kD protein	85	80/85	not assigned.no ontology/ Sec
AT1G71500.1	Rieske (2Fe-2S) domain-containing protein	64	63/–	misc. other Ferredoxins and Rieske domain/ not assigned
AT2G01140.1	Aldolase superfamily protein	42	41/40	PS.calvin cycle.aldolase/ not assigned
AT2G17630.1	Pyridoxal phosphate-dependent transferase superfamily protein	51	50/–	amino acid metabolism.synthesis.Ser-Gly-Cys group.Ser.phospho-Ser aminotransferase/ not assigned
AT4G02530.1	Chloroplast thylakoid lumen protein	74	39/74	not assigned.no ontology/ Tat
AT4G04020.1	FIB/fibrillin	56	56/56	cell.organization/ not assigned
AT4G05180.1	PSBQ, PSBQ-2, PSII-Q/PSII subunit Q-2	83	49/85	PS.lightreaction.photosystem II.PSII polypeptide subunits/ Tat
AT4G09650.1	ATPD/ATP synthase δ-subunit gene	48	49/–	PS.lightreaction.ATP synthase.delta chain/ not assigned
AT4G21280.1	PSBQ, PSBQA, PSBQ-1/PSII subunit QA	76	45/78	PS.lightreaction.photosystem II.PSII polypeptide subunits/ Tat
AT5G42650.1	AOS, CYP74A, DDE2/allene oxide synthase	34	33/22	hormone metabolism.jasmonate.synthesis-degradation.allene oxidase synthase/ not assigned

Table III. *Correctly processed plastid proteins identified with TAILS in ppi2 (other chloroplast proteins)*

Chloroplast proteins are listed that were identified in their mature (i.e. correctly processed) form on the basis of their N-terminal peptides in *ppi2*. Most processing events of nucleus-encoded plastid proteins are consistent with the ChloroP prediction, arguing for functional import and functional processing peptidases. Proteins were classified into pathways using MapMan (Thimm et al., 2004).

Identifier	Description	Start, TAILS	Start, ChloroP	MapMan Classification
AT1G09795.1	ATATP-PRT2, HISN1B, ATP-PRT2/ATP phosphoribosyl transferase2	57	58	amino acid metabolism.synthesis.His.ATP phosphoribosyl transferase
AT1G24360.1	NAD(P)-binding Rossmann-fold superfamily protein	60	58	lipid metabolism.FA synthesis and FA elongation.ACP oxoacyl reductase
AT1G73110.1	P-loop-containing nucleoside triphosphate hydrolase superfamily protein	41	40	PS.calvin cycle.Rubisco interacting
AT2G14880.1	SWIB/MDM2 domain superfamily protein	46	44	not assigned.no ontology
AT2G28000.1	CPN60A, CH-CPN60A, SLP/chaperonin-60α	47	46	PS.calvin cycle.Rubisco interacting
AT2G35500.1	SKL2/shikimate kinase-like2	71	72	amino acid metabolism.synthesis.aromatic aa.chorismate.shikimate kinase
AT2G37660.1	NAD(P)-binding Rossmann-fold superfamily protein	70	70	not assigned.unknown
AT3G08740.1	Elongation factor P (EF-P) family protein	52	51	protein.synthesis.elongation
AT3G21200.1	PGR7/proton gradient regulation7	43	42	not assigned.unknown
AT3G25920.1	RPL15/ribosomal protein L15	68	66	protein.synthesis.ribosomal protein. prokaryotic.chloroplast.50S subunit.L15
AT3G32930.1	Unknown protein	63	62	not assigned.unknown
AT3G58010.1	PGL34/plastoglobulin 34 kD	56	54	not assigned.unknown
AT3G61440.1	ATCYSC1, ARATH;BSAS3;1, CYSC1/Cys synthase C1	26	25	amino acid metabolism.synthesis. Ser-Gly-Cys group.Cys.OASTL
AT4G01310.1	Ribosomal L5P family protein	43	40	protein.synthesis.ribosomal protein. prokaryotic.chloroplast.50S subunit.L5
AT4G14680.1	APS3/pseudouridine synthase/archaeosine transglycosylase-like family protein	51	50	S-assimilation.ATPS
AT4G21445.1	Unknown protein	55	54	not assigned.unknown
AT4G23940.1	FtsH extracellular protease family	55	54	protein.degradation.metalloprotease
AT4G25370.1	Double Clp-N motif protein	65	64	protein.targeting.unknown
AT4G26900.1	AT-HF, HISN4/HIS HF	57	56	amino acid metabolism.synthesis.His. N-5-phosphoribosyl-formimino-5-aminoimidazole-4-carboxamide ribonucleotide isomerase
AT4G34350.1	CLB6, ISPH, HDR/4-hydroxy-3-methylbut-2-enyl diphosphate reductase	40	39	secondary metabolism.isoprenoids. nonmevalonate pathway.HDR
AT5G03370.1	Acylphosphatase family	67	65	not assigned.no ontology
AT5G23040.1	CDF1/protein of unknown function (DUF3353)	49	48	cell.cell death.plants
AT5G30510.1	RPS1, ARRPS1/ribosomal protein S1	45	44	protein.synthesis.ribosomal protein. prokaryotic.unknown organellar.30S subunit.S1
AT5G51110.1	Transcriptional coactivator/pterin dehydratase	51	51	not assigned.unknown
AT5G52840.1	NADH-ubiquinone oxidoreductase-related	12	11	mitochondrial electron transport / ATP synthesis.NADH-DH.localization not clear
AT5G52920.1	PKP1, PKP-β1, PKP2/plastidic pyruvate kinase β-subunit 1	65	64	glycolysis.plastid branch.pyruvate kinase (PK)
AT5G54770.1	THI1, TZ, THI4/thiazole biosynthetic enzyme, chloroplast (ARA6, THI1, THI4)	47	46	Cofactor and vitamine metabolism.thiamine
AT5G54810.1	TSB1, TRPB, TRP2, ATTSB1/Trp synthase β-subunit 1	54	53	amino acid metabolism.synthesis.aromatic aa.Trp.Trp synthase
AT5G63980.1	SAL1, ALX8, ATSAL1, HOS2, FRY1, RON1/inositol monophosphatase family protein	56	54	nucleotide metabolism.degradation
AT5G66120.2	3-Dehydroquinate synthase, putative	60	59	amino acid metabolism.synthesis.aromatic aa.chorismate.3-dehydroquinate synthase

thermolysin-treated *tic56-1* sample, indicating that these proteins were fully imported and, therefore, protected against proteolysis (Supplemental Fig. S4A). Some of the chloroplast proteins from the *tic56-1* TAILS experiment recurred in this analysis, including 29 proteins that were found correctly processed by TAILS (Tables II–V; Supplemental Table S3). Together, 225 plastid proteins were identified (Supplemental Table S3) in addition to

Table IV. *Correctly processed plastid proteins identified with TAILS in tic56-1 (thylakoid proteins)*

Chloroplast proteins are listed that were identified in their mature (i.e. correctly processed) form on the basis of their N-terminal peptides in *tic56-1*. Most processing events of nucleus-encoded plastid proteins are consistent with the ChloroP prediction or the UniProt entry for thylakoid lumenal proteins, arguing for functional import and functional processing peptidases. Thylakoid proteins were classified according to AT_CHLORO (Ferro et al., 2010). Proteins were classified into pathways using MapMan (Thimm et al., 2004).

Identifier	Description	Start, TAILS	Start, ChloroP/UniProt	MapMan Classification/Thylakoid Import Pathway
AT1G03130.1	PSAD-2/PSI subunit D-2	45	44/45	PS.lightreaction.photosystem I.PSI polypeptide subunits/ not assigned
AT1G03600.1	PSB27/PSII family protein	69	68/69	PS.lightreaction.photosystem II.PSII polypeptide subunits/ Tat
AT1G54780.1	TLP18.3/thylakoid lumen 18.3-kD protein	85	80/85	not assigned.no ontology/ Sec
AT1G71500.1	Rieske (2Fe-2S) domain-containing protein	64	63/–	misc. other Ferredoxins and Rieske domain/ not assigned
AT2G01140.1	Aldolase superfamily protein	41	41/40	PS.calvin cycle.aldolase/ not assigned
AT2G17630.1	Pyridoxal phosphate-dependent transferases superfamily protein	51	50/–	amino acid metabolism.synthesis. Ser-Gly-Cys group.Ser.phospho-Ser aminotransferase/ not assigned
AT3G44880.1	ACD1, LLS1, PAO/pheophorbide *a* oxygenase family protein with Rieske [2Fe-2S] domain	50	50/50	cell.cell death.plants/ not assigned
AT3G56650.1	Mog1/PsbP/DUF1795-like PSII reaction center PsbP family protein	68	66/68	PS.lightreaction.photosystem II.PSII polypeptide subunits/ Tat
AT3G57560.1	NAGK/*N*-acetyl-l-Glu kinase	50	50/51	nucleotide metabolism.phosphotransfer and pyrophosphatases.misc/ not assigned
AT4G02530.1	Chloroplast thylakoid lumen protein	74	39/74	not assigned.no ontology/ Tat
AT4G02770.1	PSAD-1/PSI subunit D-1	46	45/46	PS.lightreaction.photosystem I.PSI polypeptide subunits/ not assigned
AT4G04020.1	FIB/fibrillin	56	56/56	cell.organization/ not assigned
AT4G05180.1	PSBQ, PSBQ-2, PSII-Q/PSII subunit Q-2	83	49/85	PS.lightreaction.photosystem II.PSII polypeptide subunits/ Tat
AT4G09650.1	ATPD/ATP synthase δ-subunit gene	48	49/–	PS.lightreaction.ATP synthase.delta chain/ not assigned
AT4G21280.1	PSBQ, PSBQA, PSBQ-1/PSII subunit QA	76	45/78	PS.lightreaction.photosystem II.PSII polypeptide subunits/ Tat
AT5G08740.1	NDC1/NAD(P)H dehydrogenase C1	53	53/53	mitochondrial electron transport / ATP synthesis.NADH-DH.type II.mitochondrial/ not assigned
AT5G23120.1	HCF136/PSII stability/assembly factor, chloroplast (HCF136)	79	61/79	PS.lightreaction.photosystem II.biogenesis/ Tat

the TAILS data. Therefore, this analysis extends the list of proteins residing in the undeveloped plastids of *tic56-1*.

Overlap of Substrates Imported by *tic56-1* and *ppi2*

It is still an open question if substrate selectivity exists at the level of the TIC complexes (e.g. if a Tic110-containing complex or different Tic20 complexes select and transport different classes of substrates). Therefore, we analyzed the list of imported proteins from *tic56-1*. Similar to a previous study with *ppi2*, the imported proteins are involved in different pathways and no functional category is overrepresented or underrepresented (Bischof et al., 2011; Tables II–V). Furthermore, we could not define any transit peptide properties (physicochemical properties, structural aspects, or sequence conservation) that would mediate a specific import of these proteins into *tic56-1*. The same is true for *ppi2* (Bischof et al., 2011; Tables II–V). Many different substrates were found to be imported, and a remarkable overlap of substrates imported by *tic56-1* and *ppi2* was observed (Fig. 4B). This is surprising, because the two mutants are blocked at different sites of the chloroplast import machinery, which suggests partial convergence of the import routes dependent on Toc159 and Tic56, supporting their joint function in a supercomplex.

Import Assays with Another Tic56-Deficient Mutant Confirm Functional Import in the Absence of Native Tic56

Taken together, our data demonstrate a remarkable import ability of the *tic56-1* mutant. For this reason, we decided to reexamine the import ability of another *tic56* mutant, *tic56-3* (Kikuchi et al., 2013), by a classical in vitro import assay using the precursor of the small subunit of Rubisco (preSSu) and the α-subunit of pyruvate dehydrogenase E1α (preE1α) as substrates. The *tic56-3* mutant has a pale-green phenotype (Kikuchi et al., 2013; Fig. 5A). In this mutant, intact full-length Tic56 is lacking but low levels of truncated (or elongated) Tic56 occur (Kikuchi et al., 2013; Figs. 1B and 5, C and D), which could explain

Table V. *Correctly processed plastid proteins identified with TAILS in tic56-1 (other chloroplast proteins)*

Chloroplast proteins are listed that were identified in their mature (i.e. correctly processed) form on the basis of their N-terminal peptides in *tic56-1*. Most processing events of nucleus-encoded plastid proteins are consistent with the ChloroP prediction, arguing for functional import and functional processing peptidases. Proteins were classified into pathways using MapMan (Thimm et al., 2004).

Identifier	Description	Start, TAILS	Start, ChloroP	MapMan Classification
AT1G05385.1	LPA19, Psb27-H1/PSII 11-kD protein-related	68	65	PS.lightreaction.photosystem II.PSII polypeptide subunits
AT1G08490.1	ATSUFS, SUFS, ATCPNIFS, ATNFS2, CPNIFS/ chloroplastic NIFS-like Cys desulfurase	38	36	signaling.in sugar and nutrient physiology
AT1G08640.1	CJD1/chloroplast J-like domain1	60	59	not assigned.unknown
AT1G09795.1	ATATP-PRT2, HISN1B, ATP-PRT2/ATP phosphoribosyl transferase2	57	58	amino acid metabolism.synthesis.His.ATP phosphoribosyl transferase
AT1G09830.1	Glycinamide ribonucleotide (GAR) synthetase	76	75	nucleotide metabolism.synthesis.purine.GAR Synthetase
AT1G19870.1	iqd32/IQ-domain32	56	59	signaling.calcium
AT1G24360.1	NAD(P)-binding Rossmann-fold superfamily protein	58	58	lipid metabolism.FA synthesis and FA elongation.ACP oxoacyl reductase
AT1G50900.1	GDC1/ankyrin repeat family protein	66	69	not assigned.unknown
AT1G55805.1	BolA-like family protein	54	51	not assigned.no ontology
AT1G67280.1	Glyoxalase/bleomycin resistance protein/ dioxygenase superfamily protein	62	64	Biodegradation of Xenobiotics. lactoylglutathione lyase
AT1G78630.1	emb1473/ribosomal protein L13 family protein	58	57	protein.synthesis.ribosomal protein. prokaryotic.chloroplast.50S subunit.L13
AT2G14880.1	SWIB/MDM2 domain superfamily protein	44	44	not assigned.no ontology
AT2G15620.1	NIR1, NIR, ATHNIR/nitrite reductase1	28	26	N-metabolism.nitrate metabolism.nitrite reductase
AT2G28000.1	CPN60A, CH-CPN60A, SLP/chaperonin-60α	46	46	PS.calvin cycle.Rubisco interacting
AT2G35040.1	AICARFT/IMPCHase bienzyme family protein	51	51	nucleotide metabolism.synthesis.purine. AICAR transformylase
AT2G35450.1	Catalytics; hydrolases	47	47	not assigned.no ontology
AT2G35500.1	SKL2/shikimate kinase-like2	71	72	amino acid metabolism.synthesis.aromatic aa.chorismate.shikimate kinase
AT2G37660.1	NAD(P)-binding Rossmann-fold superfamily protein	70	70	not assigned.unknown
AT2G40490.1	HEME2/uroporphyrinogen decarboxylase	37	36	tetrapyrrole synthesis.uroporphyrinogen decarboxylase
AT2G44650.1	CHL-CPN10, CPN10/chloroplast chaperonin10	42	40	protein.folding
AT2G45290.1	Transketolase	67	66	PS.calvin cycle.transketolase
AT3G07480.1	2Fe-2S ferredoxin-like superfamily protein	27	26	not assigned.unknown
AT3G08740.1	Elongation factor P (EF-P) family protein	52	51	protein.synthesis.elongation
AT3G10670.1	ATNAP7, NAP7/nonintrinsic ABC protein7	67	67	protein.assembly and cofactor ligation
AT3G14210.1	ESM1/epithiospecifier modifier1	29	28	secondary metabolism.sulfur-containing. glucosinolates.degradation.myrosinase
AT3G21200.1	PGR7/proton gradient regulation7	43	42	not assigned.unknown
AT3G25920.1	RPL15/ribosomal protein L15	66	66	protein.synthesis.ribosomal protein. prokaryotic.chloroplast.50S subunit.L15
AT3G32930.1	Unknown protein	62	62	not assigned.unknown
AT3G48420.1	Haloacid dehalogenase-like hydrolase (HAD) superfamily protein	67	66	not assigned.no ontology
AT3G51140.1	Protein of unknown function (DUF3353)	69	67	not assigned.unknown
AT3G54660.1	GR, EMB2360, ATGR2/glutathione reductase	75	74	redox.ascorbate and glutathione.glutathione
AT3G58010.1	PGL34/plastoglobulin 34 kD	56	54	not assigned.unknown
AT3G58140.1	Phenylalanyl-tRNA synthetase class IIc family protein	54	54	protein.aa activation.Phe-tRNA ligase
AT3G58990.1	IPMI1/isopropylmalate isomerase1	57	57	secondary metabolism.sulfur-containing. glucosinolates.synthesis.aliphatic. methylthioalkylmalate isomerase small subunit (MAM-IS)
AT3G61440.1	ATCYSC1, ARATH;BSAS3;1, CYSC1/Cys synthase C1	26	25	amino acid metabolism.synthesis.Ser-Gly-Cys group.Cys.OASTL
AT4G01310.1	Ribosomal L5P family protein	43	40	protein.synthesis.ribosomal protein. prokaryotic.chloroplast.50S subunit.L5

(*Table continues on following page.*)

Table V. (*Continued from previous page.*)

Identifier	Description	Start, TAILS	Start, ChloroP	MapMan Classification
AT4G03200.1	Catalytics	62	62	not assigned.unknown
AT4G17560.1	Ribosomal protein L19 family protein	72	72	protein.synthesis.ribosomal protein. prokaryotic.chloroplast.50S subunit.L19
AT4G21445.1	Unknown protein	55	54	not assigned.unknown
AT4G25370.1	Double Clp-N motif protein	65	64	protein.targeting.unknown
AT4G25840.1	GPP1/glycerol-3-phosphatase1	56	54	N-metabolism.ammonia metabolism. unspecified
AT4G26900.1	AT-HF, HISN4/HIS HF	56	56	amino acid metabolism.synthesis.His.N-5-phosphoribosyl-formimino-5-aminoimidazole-4-carboxamide ribonucleotide isomerase
AT4G30490.1	AFG1-like ATPase family protein	66	67	not assigned.no ontology
AT5G01600.1	ATFER1, FER1/ferretin1	49	48	metal handling.binding, chelation and storage
AT5G03370.1	Acylphosphatase family	65	65	not assigned.no ontology
AT5G23040.1	CDF1/protein of unknown function (DUF3353)	49	48	cell.cell death.plants
AT5G30510.1	RPS1, ARRPS1/ribosomal protein S1	45	44	protein.synthesis.ribosomal protein. prokaryotic.unknown organellar.30S subunit.S1
AT5G47190.1	Ribosomal protein L19 family protein	72	72	protein.synthesis.ribosomal protein. prokaryotic.chloroplast.50S subunit.L19
AT5G48300.1	ADG1, APS1/ADP Glc pyrophosphorylase1	72	71	major CHO metabolism.synthesis.starch. AGPase
AT5G51110.1	Transcriptional coactivator/pterin dehydratase	51	51	not assigned.unknown
AT5G52840.1	NADH-ubiquinone oxidoreductase-related	12	11	mitochondrial electron transport / ATP synthesis.NADH-DH.localization not clear
AT5G52920.1	PKP1, PKP-β1, PKP2/plastidic pyruvate kinase β-subunit 1	65	64	glycolysis.plastid branch.pyruvate kinase (PK)
AT5G54770.1	THI1, TZ, THI4/thiazole biosynthetic enzyme, chloroplast (ARA6, THI1, THI4)	46	46	Cofactor and vitamine metabolism.thiamine
AT5G54810.1	TSB1, TRPB, TRP2, ATTSB1/Trp synthase β-subunit 1	54	53	amino acid metabolism.synthesis.aromatic aa.Trp.Trp synthase
AT5G63980.1	SAL1, ALX8, ATSAL1, HOS2, FRY1, RON1/ inositol monophosphatase family protein	56	54	nucleotide metabolism.degradation
AT5G66120.2	3-Dehydroquinate synthase, putative	59	59	amino acid metabolism.synthesis.aromatic aa.chorismate.3-dehydroquinate synthase

the mild phenotype when compared with *tic56-1*. We chose this mutant because, in contrast to *tic56-1*, intact Tic56-deficient chloroplasts can be isolated. Thus, the role of Tic56 in chloroplast import can be assessed directly by in vitro import studies with *tic56-3* chloroplasts. We could not observe any drastic import defect of *tic56-3* plastids for the two substrates tested (Fig. 5A), although no intact Tic56 and only low levels of modified Tic56 could be detected in the plastids used for the import reactions by western blotting (Fig. 5, C and D). Our data differ from those in the study of Kikuchi et al. (2013), who found that the import rate of preSSu-dihydrofolate reductase into *tic56-3* chloroplasts was somewhat reduced. Therefore, we chose a protoplast-based assay as a second test to assess the import capacity of *tic56-3* plastids.

Here, protoplasts of the wild type and *tic56-3* were transformed with plasmids coding for the most N-terminal amino acids of three different import substrates fused to enhanced GFP (eGFP) under the control of the strong cauliflower mosaic virus 35S promotor. We employed eGFP fusions of Arabidopsis SSu (amino acids 1–100), the α-subunit of pyruvate dehydrogenase E1α (Arabidopsis E1α; amino acids 1–100), and ferredoxin-NADP$^+$-oxidoreductase (spinach [*Spinacia oleracea*] FNR; amino acids 1–55). As control, protoplasts were transformed with a plasmid coding for eGFP only. Twenty hours after transformation, the eGFP signals of all three import substrates localized nearly completely within the chloroplasts in wild-type as well as *tic56-3* protoplasts (Fig. 6A). Western-blot analyses of protoplast protein extracts with anti-GFP revealed no difference in the migration pattern of the substrates between the wild type and *tic56-3* (Fig. 6B). In both samples, the substrates were running at the expected sizes of the processed forms lacking the transit peptide (Fig. 6B, anti GFP, triangles). In protoplasts transformed with SSu(1-100)eGFP, extra bands were detected with anti-GFP, which are most likely the result of successive degradation of the artificial import substrate inside plastids. We monitored the level of Tic56 in the transformed protoplasts by western blotting with anti-Tic56 antiserum and detected only the truncated form of Tic56 at drastically reduced levels when compared with Tic56 detected in the wild-type samples (Fig. 6B, anti Tic56). The faint band detected with anti-Tic56 in the

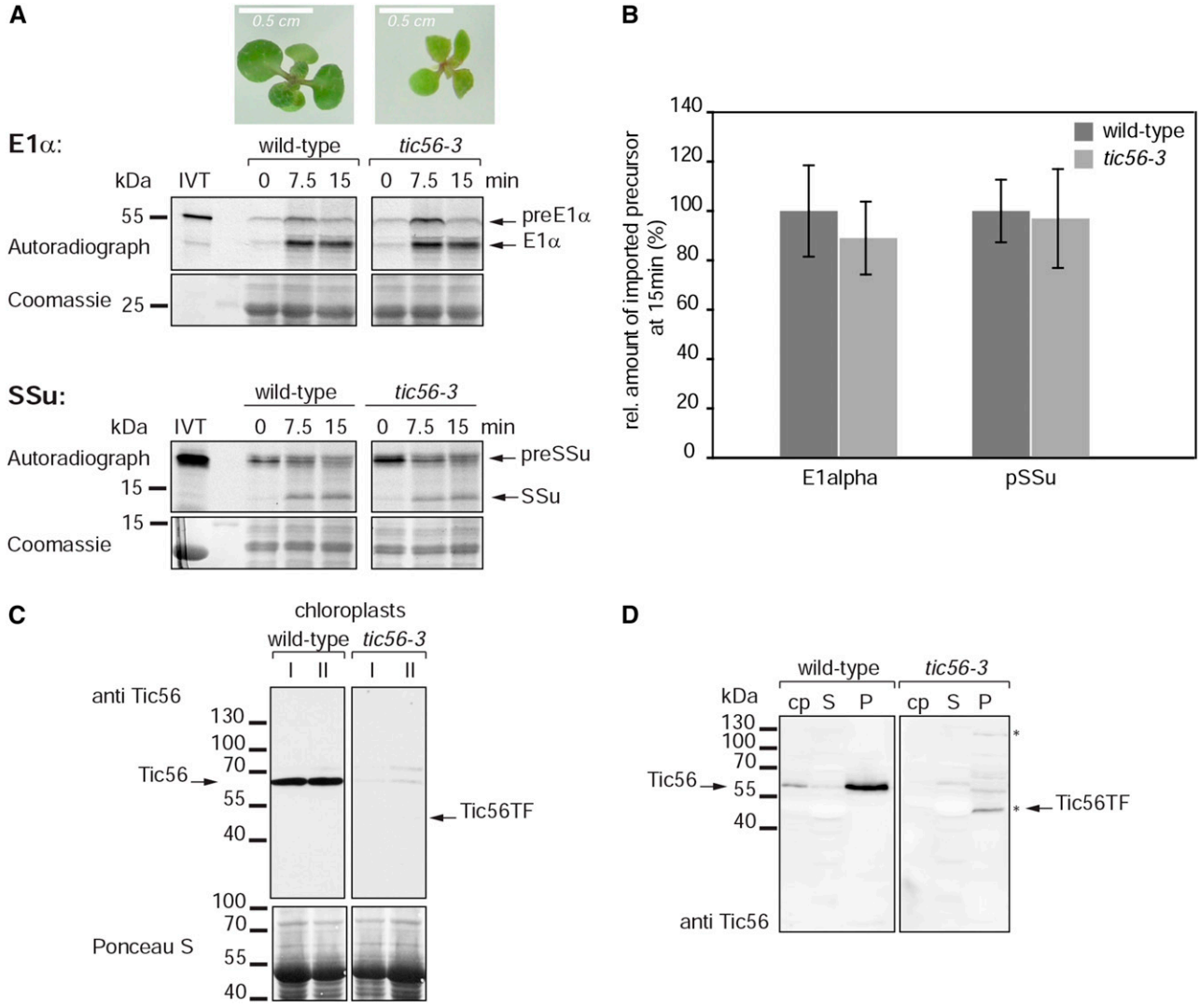

Figure 5. Import ability of chloroplasts isolated from the pale-green *tic56-3* mutant. A, In vitro chloroplast protein import assay with chloroplasts isolated from 27-d-old wild-type and *tic56-3* seedlings. For the import reactions, the chloroplast suspensions of the two plant types were adjusted to equal protein levels. The chloroplasts were incubated with two different radiolabeled import substrates, preE1α (top) and preSSu (bottom), and import was allowed to proceed for 0, 7.5, or 15 min. The samples were analyzed by SDS-PAGE and autoradiography. As a loading control, part of the Coomassie Blue-stained SDS-PAGE gel is shown underneath the corresponding autoradiograph. IVT, Product of in vitro translation. The photographs above the gels show the phenotypes of the *tic56-3* Arabidopsis mutant in comparison with the wild type (ecotype Wassilewskija) grown on Murashige and Skoog (MS) agar supplemented with 0.8% (w/v) Suc for 14 d under an 8-h photoperiod. B, Quantification of the imported, processed form of the substrates at 15 min of import. The amount of imported substrate in the wild-type sample was set to 100%. Data were derived from three independent experiments. C, Chloroplasts isolated from 27-d-old *tic56-3* seedlings have strongly reduced levels of Tic56 or the truncated form of Tic56 as monitored by western blotting. Fifty micrograms of chloroplast protein of *tic56-3* and wild-type chloroplasts from two independent preparations was analyzed by western blotting with anti-Tic56 antiserum. D, Chloroplast were lysed hypotonically and separated into soluble (S) and membrane protein (P) fractions by centrifugation. Chloroplasts (cp) and subfractions were subjected to western-blot analysis with anti-Tic56 antiserum. The 130-kD protein and the truncated form of Tic56 (Tic56-TF) became apparent in the membrane protein fraction of *tic56-3* chloroplasts (asterisks; compare with Fig. 1B, 16-d-old plants).

tic56-3 samples running at the same size of Tic56 represents a cross reaction of the antiserum with a stromal protein (Fig. 5D). All in all, our data demonstrate that, despite the high expression level of precursor proteins and the lack of Tic56 in *tic56-3* protoplasts, the substrates tested were efficiently imported into chloroplasts and did not accumulate as unprocessed precursor proteins in the cytosol. This is in line with the in vitro chloroplast import assays (Fig. 5) and the *tic56-1* TAILS data (Fig. 4; Tables II–V), thus arguing for functional import in the absence of Tic56 and, in case of *tic56-1*, in the absence of the 1-MD complex. Therefore, our data illustrate the complexity of the plastid import machinery and suggest that alternative TOC/TIC import supercomplexes exist or may form.

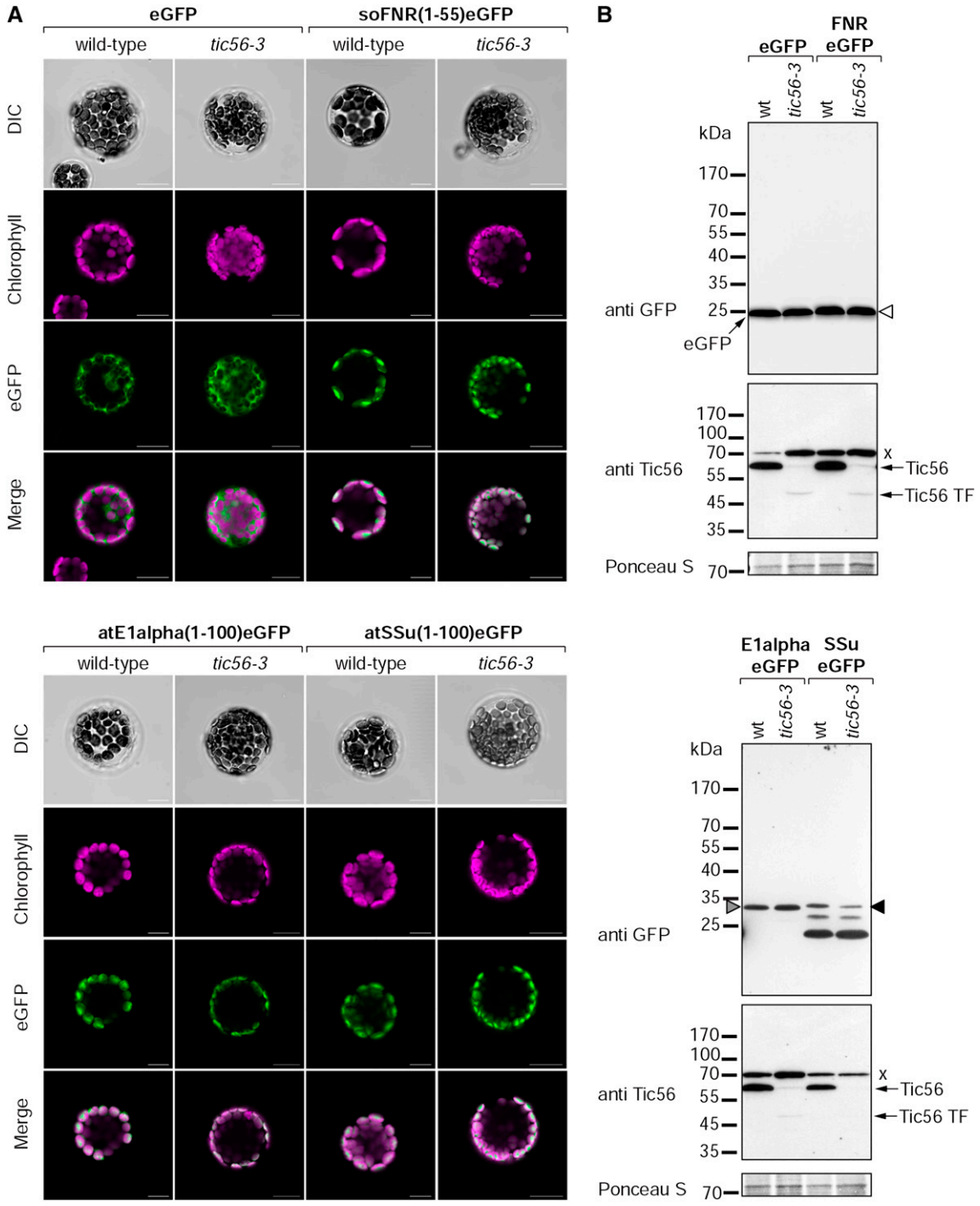

Figure 6. In vivo chloroplast targeting of three different import substrates in wild-type (wt) and *tic56-3* protoplasts. A, Arabidopsis protoplasts were transformed with constructs encoding eGFP or N-terminal fragments of spinach FNR (amino acids 1–55), E1α (amino acids 1–100), and SSu (amino acids 1–100) fused to eGFP. The localization of the reporter proteins was examined by confocal laser scanning microscopy 20 h after transformation. Chlorophyll, Chlorophyll autofluorescence; DIC, differential interference contrast; eGFP, eGFP fluorescence; Merge, superposition of chlorophyll and eGFP signals. Bars = 10 μm. B, Western-blot analysis of transformed protoplasts with an anti-GFP antibody and anti-Tic56 antiserum. A section of the Ponceau S-stained membrane is shown as a loading control. The triangles mark bands running at the expected sizes of the processed forms of the three substrates [white, eGFP; gray, E1α(62-100)eGFP; black, SSu(55-100)eGFP]. Each x indicates a nonspecific cross reaction of the anti-Tic56 antiserum with a 70-kD protein (Fig. 1B).

DISCUSSION

Protein Import in the Absence of Tic56 Disagrees with the Model of a General TIC Translocon

During precursor protein import, the TOC complexes associate with TIC complexes in the inner envelope membrane to form TOC-TIC supercomplexes that allow the translocation of protein substrates across the two membranes (Schnell et al., 1994; Kouranov et al., 1998). In this study, we provide additional evidence for the formation of TOC-TIC supercomplexes. We were able to isolate Toc159 in association with several different TIC components in the absence of precursor protein (Fig. 1). Our data, therefore, confirm that TOC-TIC supercomplexes exist independently of precursor protein translocation (Kouranov et al., 1998). The organization of the TIC complexes that associate with TOC into such supercomplexes is currently not understood. Tic20 assembles into a 1-MD translocation complex, at the inner membrane of which new subunits were recently identified (Kikuchi et al., 2013). In earlier studies, Tic20 was found in TOC-TIC supercomplexes together with Tic110, Tic40, and Tic22 (Kouranov et al., 1998). Tic110, an essential TIC component, was proposed to have a function as a translocation channel (Heins et al., 2002). However, structural data (Tsai et al., 2013) argue against this. It is more certain that Tic110 together with the cochaperone Tic40 has a role in the recruitment of stromal chaperones to the import sites (Chou et al., 2006). Initially, it was suggested that the Tic20 complex functions between the TOC complex and a Tic110 complex comprising Tic110, Tic40, and chaperones in preprotein translocation (Kikuchi et al., 2009). However, in a more recent study, Kikuchi et al. (2013) challenge a direct participation of Tic110 in the translocation process and propose the 1-MD Tic20 complex as the TIC translocon. This denomination is mainly based on the observation that Tic110 is absent in the Tic20 complex and does not comigrate in native PAGE (Kikuchi et al., 2013). Our findings support earlier data showing that Tic110 and Tic40 are part of the translocon. Our data could be explained by an association of Tic20 with Tic110 mediated by the TOC complex, which has been observed before (Kouranov et al., 1998), and point to a dynamic formation of the TOC-TIC supercomplexes (Paila et al., 2014). However, we cannot exclude the possibility that the TAP-Toc159 preparation contains different Toc159 complexes, one with Tic110 and Tic40 and a separate one with the 1-MD TIC complex. If this is the case, it would be an interesting task to determine what controls the association of the TOC complex with one or the other TIC complex.

The flexibility of the chloroplast import machinery is further reflected by our data on the protein import ability of the *tic56-1* mutant. We find a remarkably high protein import capability into plastids of *tic56-1* plants, despite the absence of the 1-MD Tic20 complex in this mutant (Kikuchi et al., 2013). This conclusion is based on the numerous correctly imported proteins identified by TAILS (Tables II–V). Thus, an intact 1-MD Tic20 complex is not necessarily required for chloroplast protein import, suggesting that its activity can be taken over by other constituents of the inner envelope membrane protein translocation machinery. This could be either the residual amounts of the unassembled components of the 1-MD complex in *tic56-1* (e.g. Tic20-I alone or its homolog Tic20-IV). Furthermore, Tic21 or a channel protein in the Tic110-Tic40-chaperone complex might have a role in maintaining the import capability in this mutant. Taken together, these results show that plastid protein translocation can take place despite the lack of Tic56 function, thus excluding the 1-MD complex as a unique TIC translocon.

Similarly, *tic56-3* plastids revealed no significant reduction in the import of different substrates in in vitro (Fig. 5) and in vivo (Fig. 6) import assays despite a shortage in Tic56. While we lack information on the state of the 1-MD TIC complex in *tic56-3*, our data clearly show that wild-type levels of native Tic56 are not required to allow for functional protein import, at least not in developed chloroplasts of plants grown under the given conditions (4 weeks old, short days). Presumably, the strong phenotype of *tic56-1* compared with *tic56-3* is caused by a default of a specific function of Tic56 during an early phase of chloroplast development that can be fulfilled by the low levels of truncated Tic56 in *tic56-3*.

A Large Variety of Substrates Is Imported in *tic56-1* and *ppi2*

As mentioned above, translocon selectivity at the level of the TOC complex has been both hypothesized and demonstrated (Jarvis et al., 1998; Bauer et al., 2000; Kubis et al., 2003, 2004; Ivanova et al., 2004; Inoue et al., 2010). However, until now, a clear classification of substrates and of sequence determinants for the different TOC import routes was unsuccessful (Bischof et al., 2011). In addition, a recent yeast (*Saccharomyces cerevisiae*) split-ubiquitin study showed that the G domains of the TOC receptors Toc159 and Toc132 can bind both photosynthetic and nonphotosynthetic precursor proteins with overlapping specificities (Dutta et al., 2014).

In view of the existence of different, separate TIC complexes, one cannot avoid the question of whether translocon selectivity also exists at the level of the TIC complex. In fact, substrate specificity at the TIC level has already been discussed for Tic20-I and Tic20-IV (Hirabayashi et al., 2011; Kasmati et al., 2011) as well as Tic21 (Teng et al., 2012), and a preference for photosynthetic precursors was attributed to Tic20-I and Tic21 (Kikuchi et al., 2009).

In the course of this work, we employed an N-terminal enrichment strategy combined with proteomics (TAILS experiment) to identify correctly imported substrates in the *tic56-1* mutant. Remarkably, many different substrates that function in various metabolic pathways were found to be imported, including several photosynthesis-related proteins (Tables II–V). Considering that Tic56 is a central component of the Tic20-I complex and is required for its integrity (Kikuchi et al., 2013), one can exclude a clear-cut

preference of this complex for photosynthetic precursor proteins. This is also supported by the in vitro import studies with the *tic56-3* mutants with different classes of import substrates (Figs. 5 and 6). A similar observation was made for *ppi2* here (Tables II–V) and in a previous report (Bischof et al., 2011), demonstrating that Toc159 contributes to the import of a broad variety of proteins and is not restricted to photosynthetic substrates.

We also found a remarkable overlap of imported proteins in the two albino mutants blocked at the TOC (*ppi2*) and TIC (*tic56-1*) levels of the translocation machinery (Fig. 4B; Tables II–V). This might suggest a common function of Toc159 and Tic56 in the same import pathway, which fits well with the occurrence of the two proteins in one TOC-TIC supercomplex as isolated from Toc159 TAP-tagged plants (Fig. 1). However, one cannot exclude that the high amount of common imported substrates detected in the two mutants is partially due to specific characteristics of the experimental system. For instance, the abundance or properties of some (N-terminal) peptides could render them more easily detectable by TAILS than others. A comparative quantitative proteomics approach with the two mutants could be helpful to complement the TAILS data.

The detection of a nucleus-encoded chloroplast peptidase (AT5G56730.1) as unprocessed precursor protein in both mutants (Table I) further points to a common function of Toc159 and Tic56. Such an accumulation of unprocessed precursor proteins in the cytosol was reported previously for Toc159-deficient *ppi2* plants (Bischof et al., 2011), and one of the precursors in that study, FERREDOXIN2 (AT1G60950.1), also was identified here in *ppi2* (Table I). A second precursor protein we found in *ppi2* only, ribosomal S5 family protein (AT2G33800.1), was classified as a Toc159-dependent substrate by Bischof et al. (2011). This agreement of the data further demonstrates the power of the TAILS approach, which identified chloroplast-localized β-amylase (AT4G17090.1) as another unprocessed precursor in *ppi2*.

The second protein identified in its unprocessed form by TAILS in *tic56-1* was a plastidic 3-phosphoglycerate dehydrogenase designated EMBRYO SAC DEVELOPMENTAL ARREST9 (EDA9; Toujani et al., 2013). The fact that the phenotype of *tic56-1* is milder than the phenotype of the *eda9* mutant (Toujani et al., 2013) indicates that the import of EDA9 is not blocked completely in *tic56-1*. EDA9 is a good candidate for an import substrate that is imported by a pathway comprising Tic56 but that is independent on Toc159. However, further experimentation is required to confirm this hypothesis.

TAILS Reveals Correct Targeting to the Thylakoid Lumen in *tic56-1* and *ppi2* and Points to a Second Proteolytic Event after Transit Peptide Removal

The power of the TAILS approach lies in its functional implications, because N termini identified in vivo provide a direct read out of either protein import with correct processing or precursor protein accumulation. We found several imported proteins in *tic56-1* and *ppi2* that were correctly processed at the predicted processing site by the stromal processing protease (SPP; Tables II–V). Furthermore, in both mutants, known thylakoid lumen-localized proteins were found whose luminal targeting signal was correctly removed (Tables II and IV). While most of these are substrates of the Tat pathway, one (AT1G54780; thylakoid lumen 18.3-kD protein) turned out to be a substrate of the Sec pathway. Therefore, our results suggest that the two albino mutants *ppi2* and *tic56-1* have functional Tat and Sec translocation pathways as well as an active thylakoid processing peptidase (plastidic type I signal peptidase1). These findings provide indirect evidence for the identity of the membrane structures observed in *tic56-1* plastids by transmission electron microscopy (Fig. 2B). The indirect evidence for the existence of a thylakoid lumen in *tic56-1* and the occurrence of plastoglobules in close proximity to the observed membrane structures support their identification as (pro)thylakoid structures. This means that *tic56-1* and *ppi2* chloroplasts, despite their severe developmental defect (Fig. 2; Supplemental Fig. S2), have the basic compartments that make up a chloroplast.

An important observation that we made with the TAILS experiment is the divergence between predicted (ChloroP) and established in vivo N termini (Fig. 4C; Supplemental Fig. S3). A similar observation was made during the development of ChloroP (Emanuelsson et al., 1999) and in proteome analyses probing the N termini of plastid proteins (Gómez et al., 2003; Zybailov et al., 2008; Huesgen et al., 2013). This interesting finding was interpreted in two different ways: on the one hand, it was attributed to the inaccuracy of the ChloroP prediction tool (Zybailov et al., 2008), and on the other hand, it was suggested that most imported chloroplast proteins undergo additional N-terminal proteolysis after transit peptide removal by SPP (Emanuelsson et al., 1999; Huesgen et al., 2013). Our data show that the starting amino acid aligns with the preferential exposure of stabilizing amino acids at the N terminus. Cys residues are removed from the N terminus, and the number of proteins starting with Ala as the first amino acid is significantly reduced compared with the ChloroP prediction (Supplemental Fig. S3B). As a result, we observed a shift in the starting amino acids from known stabilizing to destabilizing residues in plastids according to Apel et al. (2010). The one-amino acid shift results in the change of the N-terminal amino acid from a strong instability-conferring amino acid (Cys) to residues that confer intermediate stability (Ser and Gly) or to the stabilizing amino acid Glu (Supplemental Fig. S3B; Apel et al., 2010). Such a second proteolytic event after SPP cleavage would be very much reminiscent of the presequence trimming of mitochondrial (pre)proteins by Icp55 (for intermediate cleaving peptidase of 55 kD) in yeast (Naamati et al., 2009; Vögtle et al., 2009). This protease exposes stabilizing residues at the N terminus of intermediate processing products generated by the mitochondrial processing peptidase, thereby determining their half-lives (Vögtle et al., 2009; Venne et al., 2013). It is conceivable that a similar proteolytic system exists in chloroplasts;

however, despite the existence of Icp55 homologs in plants (Kwasniak et al., 2012), a plastid-localized Icp55-like protease remains to be discovered.

CONCLUSION

Altogether, our results provide further evidence for a role of Tic56 in chloroplast protein translocation (Kikuchi et al., 2013). This is supported by its interaction with Toc159 and the intersection of substrates that are imported or not in *tic56-1* and the protein import mutant *ppi2*. However, the *tic56-1* TAILS data and the import studies with *tic56-3* argue against a function of Tic56 as an essential component of a unique general TIC translocon, because considerable import was observed despite Tic56 deficiency. Our results also demonstrate that TAILS is a powerful tool to study plastid or mitochondrial protein import in mutants whose severe phenotype (e.g. albino, dwarf) hamper classical approaches such as in vitro protein import assays.

MATERIALS AND METHODS

Plant Material and Growth Conditions

The following Arabidopsis (*Arabidopsis thaliana*) mutants were used: *tic56-1* (SAIL_810_G07), *tic56-3* (FLAG_579H12), and *ppi2* (*toc159*; *CS11072* introgressed into the Columbia-0 ecotype; Kubis et al., 2004). As control, wild-type plants of the ecotypes Wassilewskija or Columbia-0 were used. Plants were grown at 21°C under short-day conditions (8-/16-h photoperiod) on agar plates. Agar plates contained 1% (w/v) plant agar, one-half-strength MS medium, and 0.8% (w/v) Suc.

TAP Tag Purification

The transgenic plants (TAP-Toc159:*ppi2*) used for the isolation of TAP-Toc159-containing complexes have been described before, as has the procedure of purification and mass spectrometry analysis (Agne et al., 2010).

DNA Constructs

To obtain a vector for Tic56 antigen production, the coding sequence for Tic56 without transit peptide was amplified with forward primer 5′-GTATAGGATCCTT-CTCAAAGAAGTCCC-3′ and reverse primer 5′-GAGTGCGGCCGCTCAATCTT-TTTTGGAGTTGC-3′ from clone RAFL05-19-G19 (pda02782; RIKEN Bioresource Center). The insert was subsequently cloned using *Bam*HI/*Not*I into pGEX-4T-2. The vector backbone of all plasmids for Arabidopsis protoplast transformation was pRT100Ω/Not/Asc (Uberlacker and Werr, 1996) containing the coding sequence of eGFP (Clontech). The plasmid pRT100Ω/Not/Asc-eGFP as well as the construct pRT100Ω/Not/Asc pRT100 encoding the first 55 amino acids of spinach (*Spinacia oleracea*) FNR fused to eGFP was kindly provided by Ralf Bernd Klösgen. The coding sequences for the first 100 residues of the SSu and E1α were cloned into pRT100Ω/Not/Asc-eGFP between the cauliflower mosaic virus 35S promotor region and the eGFP coding sequence. For in vitro transcription/translation of chloroplast precursor proteins, the complementary DNAs of E1α and SSu were cloned using *Nco*I/*Sal*I into pET21d. An internal *Nco*I site in the complementary DNA of the small subunit was mutated by site-directed mutagenesis with forward primer 5′-CCGGCTCAAGCCACGATGGTCGCTCCATTCACTGG-3′ and reverse primer 5′-CCAGTGAATGGAGCGACCATCGTGGCTTGAGCCGG-3′.

Anti-Tic56 Antiserum Production

A fusion protein of glutathione *S*-transferase (GST) and Tic56 without transit peptide (amino acids 48–527) was overexpressed in *Escherichia coli* BL21 (DE3). Inclusion bodies were prepared according to the method described by Palmer and Wingfield (2012). Proteins of the inclusion bodies were separated on a gradient SDS-PAGE (5%–12% acrylamide), and the most intensive bands after Coomassie Blue staining were cut out. The presence of the GST-Tic56 antigen in these slices was confirmed by mass spectrometry. The gel slices were sent to Eurogentec for polyclonal antibody production.

Protein Extraction and Immunoblotting

The plant material was shock frozen in liquid nitrogen and ground to a fine powder. Protein extraction buffer (100 mM sodium chloride, 50 mM Tris, pH 7.5, 4% [w/v] SDS, 0.1% [v/v] plant protease inhibitor cocktail [Sigma-Aldrich], and 1 mM phenylmethylsulfonyl fluoride) was added, and the samples were incubated for 10 min at 70°C while shaking. The samples were clarified by centrifugation at maximum speed in a tabletop centrifuge for 10 min at room temperature. The protein content was determined using the bicinchoninic acid assay (Serva), and proteins were chloroform/methanol precipitated (Wessel and Flügge, 1984). For SDS-PAGE, the protein pellets were dissolved in SDS sample buffer and incubated at 95°C for 5 min. Subsequent to separation by SDS-PAGE, the proteins were transferred to polyvinylidene difluoride membranes by semidry blotting (Kyhse-Andersen, 1984) or to nitrocellulose by tank blotting using Dunn carbonate buffer. Anti-Lhcb2, anti-Lhcb4, anti-RbcS, anti-PsbA, and anti-Tic40 sera were purchased from Agrisera, and monoclonal anti-actin (A0480) and monoclonal anti-GFP (G6795) sera were from Sigma-Aldrich. Other primary antibodies and antisera used in this study include anti-atTic56 (this study), anti-atTic20 (Teng et al., 2006), anti-atToc33 (Agne et al., 2009), anti-atToc75 (Hiltbrunner et al., 2001b), anti-atToc132 (from D.J. Schnell, University of Massachusetts), anti-atToc159 (Bauer et al., 2000), anti-atPgl35 (Vidi et al., 2006), and anti-atTic110 (Bauer et al., 2000). Band intensities of blots were quantified using ImageJ software (National Institutes of Health).

Transmission Electron Microscopy

Leaf segments were fixed with 3% (v/v) glutaraldehyde in sodium cacodylate buffer (SCB), pH 7.2, for 4 h at room temperature, washed with SCB, postfixed with 1% (w/v) osmium tetroxide in SCB for 1 h, dehydrated in a graded ethanol series, and embedded in epoxy resin (Spurr, 1969). After polymerization, the material was sectioned with an ultramicrotome S (Leica). Semithin sections (1 μm) were stained with 1% (w/v) Toluidine Blue and observed with an Axioskop 20 light microscope (Carl Zeiss Microscopy). Ultrathin sections (80 nm) were transferred to coated copper grids and poststained with uranyl acetate and lead citrate. The sections were observed using a LIBRA 120 device (Carl Zeiss Microscopy) operating at 120 kV. Images were taken applying a Dual-Speed on axis SSCCD camera (BM-2k-120; TRS).

Transient Expression of eGFP Fusion Proteins in Arabidopsis Protoplasts

Protoplast isolation and transformation were done using a polyethylene glycol-based method adapted from the protocols of Jin et al. (2001) and Yoo et al. (2007). Twenty-six-day-old wild-type (Wassilewskija) and *tic56-3* plants grown on agar plates were harvested in enzyme buffer without enzymes (400 mM sorbitol, 5 mM MES, and 8 mM calcium chloride, pH 5.6). After cutting the leaves with a razor blade, the buffer was replaced by the same buffer containing 1.5% (w/v) Cellulase Onozuka R-10 (Serva) and 0.375% (w/v) Macerozyme R-10 (Serva). After two vacuum infiltration steps (5 min, −800 mbar), digestion was allowed to proceed for 4 h at room temperature. Protoplasts were collected by gentle shaking, filtering through a 50-μm mesh, and centrifugation for 5 min at 100*g*. Protoplasts were washed once in 5 to 15 mL of W5 solution (154 mM sodium chloride, 125 mM calcium chloride, 5 mM potassium chloride, 5 mM Glc, and 1.5 mM MES, pH 5.6) and resuspended in cold W5 solution to a final concentration of 2×10^6 protoplasts mL^{-1}. After incubation for 30 min on ice, the protoplasts were sedimented by centrifugation and resuspended in the same volume of MaMg solution (400 mM sorbitol, 15 mM magnesium chloride, and 5 mM MES, pH 5.6). For each transformation, 400 μL of protoplast suspension was combined with 40 μg of plasmid and subsequently carefully mixed with 440 μL of PEG-CMS (1 g of polyethylene glycol 4000, 375 μL of water, 1 mL of 500 mM sorbitol, and 250 μL of 1 M calcium nitrate). After incubation for 20 min at room temperature, the protoplasts were washed by stepwise addition of W5 solution and centrifugation for 2 min with 100*g*. The protoplasts were washed in 4 mL of protoplast culture medium (4.4 g L^{-1} MS medium, 350 mM sorbitol, 50 mM Glc, 3 mM calcium chloride, and 50 μg mL^{-1} ampicillin, pH 5.8) and finally resuspended in 2 mL of protoplast culture medium. After an incubation of approximately 20 h, the samples

were analyzed using confocal laser scanning microscopy. Twenty-four hours after transformation, protoplast were collected by centrifugation for 5 min at 500*g* and resuspended in 50 mM Tris-HCl, pH 6.8, 10 mM dithiothreitol, and 0.2% (v/v) plant protease inhibitor cocktail P9599 (Sigma-Aldrich) prior to chloroform/methanol precipitation (Wessel and Flügge, 1984). Fifty micrograms of protoplast protein was used for anti-GFP and anti-Tic56 western-blot analyses.

Confocal Laser Scanning Microscopy

Protoplasts were observed using a Plan-Apochromat 40×/0.95 objective on an LSM-780 confocal microscope (Zeiss). The chlorophyll fluorescence was excited with a helium-neon laser (633 nm) and the eGFP with an argon laser (488 nm). Emission wavelengths were 647 to 721 nm for chlorophyll and 493 to 598 nm for eGFP. Data from both channels were collected simultaneously in one scan event. After acquisition, images were processed using Carl Zeiss ZEN lite 2012 software.

TAILS

TAILS was done in two experiments with two biological replicates for *tic56-1* compared with the wild type. In the second experiment, the *ppi2* mutant was analyzed in addition. First, total protein was extracted from 8-week-old plant material. Plant material was frozen in liquid nitrogen and ground with a pestle. In the first experiment, HEPES/NaOH buffer (pH 7) was added; in the second experiment, the buffer contained additionally 0.1% (v/v) plant protease inhibitor cocktail from Sigma-Aldrich, 1 mM phenylmethylsulfonyl fluoride, and 4% (w/v) SDS to solubilize membrane proteins. The extract was clarified from the remaining plant material by centrifugation. From each plant line, 100 μg of total protein was used for further steps. The N-terminal blocking, protein digestion, peptide filtering, and sample desalting were done as described (Doucet et al., 2011). In the first experimental setup, the protein samples from both plant lines were blocked using different isotopes of formaldehyde (wild type, $^{12}C^{1}H_2O$; *tic56-1*, $^{13}C^{2}H_2O$). Afterward, both samples were combined and treated together in further steps. In the second experimental setup, all three protein samples were blocked using normal formaldehyde and treated separately. The samples were analyzed on an LTQ Orbitrap Velos device (Thermo Scientific). The desalted and completely dried samples were resuspended in water with 2% (v/v) acetonitrile and 0.1% (v/v) formic acid. Samples were separated by liquid chromatography using C18 columns from Proxeon (guard column, 2 cm, with i.d. of 100 μm, 5 μm; analytical column, 10 cm, with i.d. of 75 μm, 3 μm). For separation, a gradient consisting of water with 0.1% (v/v) formic acid (A) and acetonitrile with 0.1% (v/v) formic acid (B) was used (0–150 min, 5%–40% B; 150–160 min, 40%–80% B; 160–170 min, 80% B). Precursor detection was done in a mass-to-charge ratio range from 400 to 1,850, and the 20 most intensive signals were used for tandem mass spectrometry.

TAILS Data Processing

The raw files were analyzed using Proteome Discoverer 1.2 (Thermo Scientific) with the search engine SEQUEST and with MaxQuant 1.3.0.5 (Cox and Mann, 2008) using the search engine Andromeda (Cox et al., 2011). In both cases, The Arabidopsis Information Resource 10 database was used, and the false discovery rate of the data set was set to 5%. As variable modifications, N-terminal acetylation and Met oxidation, and as fixed modifications, carbamidomethylation of Cys, dimethylation of N termini or on Lys side chains, originating from the blocking procedure, were allowed. In Proteome Discoverer, the precursor mass tolerance was set to 7 ppm and the fragment mass tolerance to 0.8 D. We accepted semitryptic peptides with a maximum number of one missed cleavage. Using MaxQuant, Lys and N-terminal dimethylation were accepted in the group-specific parameters table as labels. The precursor mass was set to an accuracy of 10 ppm and the fragment mass to 0.5 D. Here, we also accepted semitryptic peptides with a maximal number of three missed cleavages. The mass spectrometry proteomics data have been deposited to the ProteomeXchange Consortium (http://proteomecentral.proteomexchange.org) via the PRIDE partner repository (Vizcaíno et al., 2013) with the data set identifier PXD000660. For further analyses, the identified peptides must have had blocked N termini by dimethylation or acetylation and had to be unique for one protein. Peptides without a C-terminal Arg or Lys as evidence for a tryptic origin were filtered out. The lists of determined peptides (Supplemental Table S1) from both experiments and all data analysis were combined for each plant line. The minimal starting position of the assigned proteins was determined using a program that detects the position of the peptides in the proteins (from Katja Bärenfaller). The mapping of the observed proteins to the organelles was done using a chloroplast reference proteome (van Wijk and Baginsky, 2011) and SUBAIII (Tanz et al., 2013). The theoretical starting position was predicted with ChloroP (Emanuelsson et al., 1999). For proteins that were assigned as thylakoid localized by AT_CHLORO (Ferro et al., 2010), the start position of the mature protein listed in the UniProt database was taken. Sequences were analyzed using WebLogo (Crooks et al., 2004).

Chloroplast Preparation and in Vitro Chloroplast Import Studies

The preparation of intact Arabidopsis chloroplasts and in vitro import were performed as described before (Agne et al., 2009). For western-blot analysis, chloroplasts corresponding to 50 μg of chlorophyll were treated or not with 50 μg mL^{-1} thermolysin in 100 μL of HS buffer (50 mM HEPES-KOH, pH 8, and 330 mM sorbitol) supplemented with 0.5 mM $CaCl_2$ for 30 min on ice. The reaction was stopped with 20 mM EDTA in HS buffer for 5 min on ice. Chloroplasts were reisolated, washed with HS buffer, and denatured in SDS-PAGE loading buffer. For fractionation into soluble and membrane proteins, chloroplasts were resuspended in 10 mM Tris-HCl, pH 8, 1 mM EDTA, 5 mM dithiothreitol, and 0.1% (v/v) plant protease inhibitor cocktail P9599 (Sigma-Aldrich) to a final chlorophyll concentration of 0.5 mg mL^{-1}. After lysis for 30 min on ice, soluble and membrane fractions were obtained by centrifugation for 30 min at 15,000*g* and 4°C. For in vitro import, chloroplasts isolated from 27-d-old wild-type and *tic56-3* mutant seedlings grown under an 8-h photoperiod were adjusted to equal amounts of protein (corresponding to 17.5 μg of chlorophyll of the wild-type chloroplasts per time point). The samples of the import reactions were resolved by SDS-PAGE and analyzed by phosphorimaging (Fujifilm; BAS1500 or BAS1800) and quantification with the Tina 2.10i software (Raytest).

Sequence data from this article can be found in the GenBank/EMBL data libraries under the following accession numbers: Rubisco (At5g38430), Lhcb4.1 (At5g01530), E1α (At1g01090), Toc159 (At4g02510), and Tic56 (At5g01590).

Supplemental Data

The following supplemental materials are available.

Supplemental Figure S1. Genotyping and gene expression analysis of the *tic56-3* mutant.

Supplemental Figure S2. Phenotypes of the mutants *ppi2* and *tic56-1* compared with the wild type.

Supplemental Figure S3. Comparison of experimental and theoretical processing sites and resulting N-terminal amino acids.

Supplemental Figure S4. Proteins of *tic56-1* plastids are protected during thermolysin treatment.

Supplemental Table S1. Summary of all proteins identified in the TAILS experiment with the minimal starting positions.

Supplemental Table S2. Summary of all peptides identified in the TAILS experiments used for further analyses.

Supplemental Table S3. Summary of unique peptides identified in the proteome analysis of *tic56-1* and wild-type plastids (thermolysin treatment).

Supplemental Methods S1. Experimental approaches for Supplemental Figures S1 and S4.

ACKNOWLEDGMENTS

We thank Paul Jarvis (University of Leicester) for providing *ppi2* in the Columbia-0 background; Julia Grimmer, Anja Rödiger, and Ralf Bernd Klösgen (Martin-Luther-University Halle-Wittenberg) for providing plasmid constructs; Hsou-min Li (Institute of Molecular Biology, Academia Sinica) for donating the anti-atTic20 antibody; the ProteomeXchange Consortium for the possibility to deposit the proteomics data; and Dr. Katja Bärenfaller (Eidgenössisch Technische Hochschule) and Dr. Dirk Dobritzsch and Nina Pötzsch (Martin-Luther-University Halle-Wittenberg) for providing tools for the determination of the minimal peptide positions and peptide positions in protein sequences, respectively.

Received December 13, 2014; accepted January 14, 2015; published January 14, 2015.

LITERATURE CITED

Agne B, Andrès C, Montandon C, Christ B, Ertan A, Jung F, Infanger S, Bischof S, Baginsky S, Kessler F (2010) The acidic A-domain of Arabidopsis TOC159 occurs as a hyperphosphorylated protein. Plant Physiol **153:** 1016–1030

Agne B, Infanger S, Wang F, Hofstetter V, Rahim G, Martin M, Lee DW, Hwang I, Schnell D, Kessler F (2009) A toc159 import receptor mutant, defective in hydrolysis of GTP, supports preprotein import into chloroplasts. J Biol Chem **284:** 8670–8679

Apel W, Schulze WX, Bock R (2010) Identification of protein stability determinants in chloroplasts. Plant J **63:** 636–650

Balsera M, Goetze TA, Kovács-Bogdán E, Schürmann P, Wagner R, Buchanan BB, Soll J, Bölter B (2009) Characterization of Tic110, a channel-forming protein at the inner envelope membrane of chloroplasts, unveils a response to Ca^{2+} and a stromal regulatory disulfide bridge. J Biol Chem **284:** 2603–2616

Bauer J, Chen K, Hiltbunner A, Wehrli E, Eugster M, Schnell D, Kessler F (2000) The major protein import receptor of plastids is essential for chloroplast biogenesis. Nature **403:** 203–207

Bischof S, Baerenfaller K, Wildhaber T, Troesch R, Vidi PA, Roschitzki B, Hirsch-Hoffmann M, Hennig L, Kessler F, Gruissem W, et al (2011) Plastid proteome assembly without Toc159: photosynthetic protein import and accumulation of *N*-acetylated plastid precursor proteins. Plant Cell **23:** 3911–3928

Chotewutmontri P, Reddick LE, McWilliams DR, Campbell IM, Bruce BD (2012) Differential transit peptide recognition during preprotein binding and translocation into flowering plant plastids. Plant Cell **24:** 3040–3059

Chou ML, Chu CC, Chen LJ, Akita M, Li HM (2006) Stimulation of transit-peptide release and ATP hydrolysis by a cochaperone during protein import into chloroplasts. J Cell Biol **175:** 893–900

Cline K, Werner-Washburne M, Andrews J, Keegstra K (1984) Thermolysin is a suitable protease for probing the surface of intact pea chloroplasts. Plant Physiol **75:** 675–678

Cox J, Mann M (2008) MaxQuant enables high peptide identification rates, individualized p.p.b.-range mass accuracies and proteome-wide protein quantification. Nat Biotechnol **26:** 1367–1372

Cox J, Neuhauser N, Michalski A, Scheltema RA, Olsen JV, Mann M (2011) Andromeda: a peptide search engine integrated into the MaxQuant environment. J Proteome Res **10:** 1794–1805

Crooks GE, Hon G, Chandonia JM, Brenner SE (2004) WebLogo: a sequence logo generator. Genome Res **14:** 1188–1190

Doucet A, Kleifeld O, Kizhakkedathu JN, Overall CM (2011) Identification of proteolytic products and natural protein N-termini by terminal amine isotopic labeling of substrates (TAILS). Methods Mol Biol **753:** 273–287

Dutta S, Teresinski HJ, Smith MD (2014) A split-ubiquitin yeast two-hybrid screen to examine the substrate specificity of atToc159 and atToc132, two Arabidopsis chloroplast preprotein import receptors. PLoS ONE **9:** e95026

Emanuelsson O, Nielsen H, von Heijne G (1999) ChloroP, a neural network-based method for predicting chloroplast transit peptides and their cleavage sites. Protein Sci **8:** 978–984

Ferro M, Brugière S, Salvi D, Seigneurin-Berny D, Court M, Moyet L, Ramus C, Miras S, Mellal M, Le Gall S, et al (2010) AT_CHLORO, a comprehensive chloroplast proteome database with subplastidial localization and curated information on envelope proteins. Mol Cell Proteomics **9:** 1063–1084

Gómez SM, Bil' KY, Aguilera R, Nishio JN, Faull KF, Whitelegge JP (2003) Transit peptide cleavage sites of integral thylakoid membrane proteins. Mol Cell Proteomics **2:** 1068–1085

Heins L, Mehrle A, Hemmler R, Wagner R, Küchler M, Hörmann F, Sveshnikov D, Soll J (2002) The preprotein conducting channel at the inner envelope membrane of plastids. EMBO J **21:** 2616–2625

Hiltbrunner A, Bauer J, Alvarez-Huerta M, Kessler F (2001a) Protein translocon at the Arabidopsis outer chloroplast membrane. Biochem Cell Biol **79:** 629–635

Hiltbrunner A, Bauer J, Vidi PA, Infanger S, Weibel P, Hohwy M, Kessler F (2001b) Targeting of an abundant cytosolic form of the protein import receptor at Toc159 to the outer chloroplast membrane. J Cell Biol **154:** 309–316

Hirabayashi Y, Kikuchi S, Oishi M, Nakai M (2011) In vivo studies on the roles of two closely related Arabidopsis Tic20 proteins, AtTic20-I and AtTic20-IV. Plant Cell Physiol **52:** 469–478

Huang S, Shingaki-Wells RN, Taylor NL, Millar AH (2013) The rice mitochondria proteome and its response during development and to the environment. Front Plant Sci **4:** 16

Huesgen PF, Alami M, Lange PF, Foster LJ, Schröder WP, Overall CM, Green BR (2013) Proteomic amino-termini profiling reveals targeting information for protein import into complex plastids. PLoS ONE **8:** e74483

Infanger S, Bischof S, Hiltbrunner A, Agne B, Baginsky S, Kessler F (2011) The chloroplast import receptor Toc90 partially restores the accumulation of Toc159 client proteins in the Arabidopsis thaliana ppi2 mutant. Mol Plant **4:** 252–263

Inoue H, Rounds C, Schnell DJ (2010) The molecular basis for distinct pathways for protein import into *Arabidopsis* chloroplasts. Plant Cell **22:** 1947–1960

Ivanova Y, Smith MD, Chen K, Schnell DJ (2004) Members of the Toc159 import receptor family represent distinct pathways for protein targeting to plastids. Mol Biol Cell **15:** 3379–3392

Ivey RA III, Subramanian C, Bruce BD (2000) Identification of a Hsp70 recognition domain within the Rubisco small subunit transit peptide. Plant Physiol **122:** 1289–1299

Jarvis P (2008) Targeting of nucleus-encoded proteins to chloroplasts in plants. New Phytol **179:** 257–285

Jarvis P, Chen LJ, Li H, Peto CA, Fankhauser C, Chory J (1998) An Arabidopsis mutant defective in the plastid general protein import apparatus. Science **282:** 100–103

Jin JB, Kim YA, Kim SJ, Lee SH, Kim DH, Cheong GW, Hwang I (2001) A new dynamin-like protein, ADL6, is involved in trafficking from the *trans*-Golgi network to the central vacuole in *Arabidopsis*. Plant Cell **13:** 1511–1526

Kasmati AR, Töpel M, Patel R, Murtaza G, Jarvis P (2011) Molecular and genetic analyses of Tic20 homologues in Arabidopsis thaliana chloroplasts. Plant J **66:** 877–889

Kikuchi S, Bédard J, Hirano M, Hirabayashi Y, Oishi M, Imai M, Takase M, Ide T, Nakai M (2013) Uncovering the protein translocon at the chloroplast inner envelope membrane. Science **339:** 571–574

Kikuchi S, Oishi M, Hirabayashi Y, Lee DW, Hwang I, Nakai M (2009) A 1-megadalton translocation complex containing Tic20 and Tic21 mediates chloroplast protein import at the inner envelope membrane. Plant Cell **21:** 1781–1797

Kleifeld O, Doucet A, auf dem Keller U, Prudova A, Schilling O, Kainthan RK, Starr AE, Foster LJ, Kizhakkedathu JN, Overall CM (2010) Isotopic labeling of terminal amines in complex samples identifies protein N-termini and protease cleavage products. Nat Biotechnol **28:** 281–288

Kouranov A, Chen X, Fuks B, Schnell DJ (1998) Tic20 and Tic22 are new components of the protein import apparatus at the chloroplast inner envelope membrane. J Cell Biol **143:** 991–1002

Kovács-Bogdán E, Benz JP, Soll J, Bölter B (2011) Tic20 forms a channel independent of Tic110 in chloroplasts. BMC Plant Biol **11:** 133

Kubis S, Baldwin A, Patel R, Razzaq A, Dupree P, Lilley K, Kurth J, Leister D, Jarvis P (2003) The *Arabidopsis ppi1* mutant is specifically defective in the expression, chloroplast import, and accumulation of photosynthetic proteins. Plant Cell **15:** 1859–1871

Kubis S, Patel R, Combe J, Bédard J, Kovacheva S, Lilley K, Biehl A, Leister D, Ríos G, Koncz C, et al (2004) Functional specialization amongst the *Arabidopsis* Toc159 family of chloroplast protein import receptors. Plant Cell **16:** 2059–2077

Kwasniak M, Pogorzelec L, Migdal I, Smakowska E, Janska H (2012) Proteolytic system of plant mitochondria. Physiol Plant **145:** 187–195

Kyhse-Andersen J (1984) Electroblotting of multiple gels: a simple apparatus without buffer tank for rapid transfer of proteins from polyacrylamide to nitrocellulose. J Biochem Biophys Methods **10:** 203–209

Lange PF, Overall CM (2013) Protein TAILS: when termini tell tales of proteolysis and function. Curr Opin Chem Biol **17:** 73–82

Li HM, Teng YS (2013) Transit peptide design and plastid import regulation. Trends Plant Sci **18:** 360–366

Ling Q, Huang W, Baldwin A, Jarvis P (2012) Chloroplast biogenesis is regulated by direct action of the ubiquitin-proteasome system. Science **338:** 655–659

Motohashi R, Rödiger A, Agne B, Baerenfaller K, Baginsky S (2012) Common and specific protein accumulation patterns in different albino/pale-green mutants reveals regulon organization at the proteome level. Plant Physiol **160:** 2189–2201

Naamati A, Regev-Rudzki N, Galperin S, Lill R, Pines O (2009) Dual targeting of Nfs1 and discovery of its novel processing enzyme, Icp55. J Biol Chem **284:** 30200–30208

Paila YD, Richardson LG, Schnell DJ (2014) New insights into the mechanism of chloroplast protein import and its integration with protein quality control, organelle biogenesis and development. J Mol Biol (in press)

Palmer I, Wingfield PT (2012) Preparation and extraction of insoluble (inclusion-body) proteins from Escherichia coli. Curr Protoc Protein Sci **Chapter 6:** Unit 6.3

Pilon M, Wienk H, Sips W, de Swaaf M, Talboom I, van't Hof R, de Korte-Kool G, Demel R, Weisbeek P, de Kruijff B (1995) Functional domains of the ferredoxin transit sequence involved in chloroplast import. J Biol Chem **270:** 3882–3893

Richly E, Dietzmann A, Biehl A, Kurth J, Laloi C, Apel K, Salamini F, Leister D (2003) Covariations in the nuclear chloroplast transcriptome reveal a regulatory master-switch. EMBO Rep **4:** 491–498

Schnell DJ, Blobel G, Keegstra K, Kessler F, Ko K, Soll J (1997) A consensus nomenclature for the protein-import components of the chloroplast envelope. Trends Cell Biol **7:** 303–304

Schnell DJ, Kessler F, Blobel G (1994) Isolation of components of the chloroplast protein import machinery. Science **266:** 1007–1012

Shi LX, Theg SM (2013) The chloroplast protein import system: from algae to trees. Biochim Biophys Acta **1833:** 314–331

Smith MD, Rounds CM, Wang F, Chen K, Afitlhile M, Schnell DJ (2004) atToc159 is a selective transit peptide receptor for the import of nucleus-encoded chloroplast proteins. J Cell Biol **165:** 323–334

Spurr AR (1969) A low-viscosity epoxy resin embedding medium for electron microscopy. J Ultrastruct Res **26:** 31–43

Tanz SK, Castleden I, Hooper CM, Vacher M, Small I, Millar HA (2013) SUBA3: a database for integrating experimentation and prediction to define the SUBcellular location of proteins in Arabidopsis. Nucleic Acids Res **41:** D1185–D1191

Teng YS, Chan PT, Li HM (2012) Differential age-dependent import regulation by signal peptides. PLoS Biol **10:** e1001416

Teng YS, Su YS, Chen LJ, Lee YJ, Hwang I, Li HM (2006) Tic21 is an essential translocon component for protein translocation across the chloroplast inner envelope membrane. Plant Cell **18:** 2247–2257

Thimm O, Bläsing O, Gibon Y, Meyer S, Krüger P, Selbig J, Müller LA, Rhee SY, Stitt M (2004) MAPMAN: a user-driven tool to display genomics data sets onto diagrams of metabolic pathways and other biological processes. Plant J **37:** 914–939

Toujani W, Muñoz-Bertomeu J, Flores-Tornero M, Rosa-Téllez S, Anoman AD, Alseekh S, Fernie AR, Ros R (2013) Functional characterization of the plastidial 3-phosphoglycerate dehydrogenase family in Arabidopsis. Plant Physiol **163:** 1164–1178

Tsai JY, Chu CC, Yeh YH, Chen LJ, Li HM, Hsiao CD (2013) Structural characterizations of the chloroplast translocon protein Tic110. Plant J **75:** 847–857

Uberlacker B, Werr W (1996) Vectors with rare-cutter restriction enzyme sites for expression of open reading frames in transgenic plants. Mol Breed **2:** 293–295

van Wijk KJ, Baginsky S (2011) Plastid proteomics in higher plants: current state and future goals. Plant Physiol **155:** 1578–1588

Venne AS, Vögtle FN, Meisinger C, Sickmann A, Zahedi RP (2013) Novel highly sensitive, specific, and straightforward strategy for comprehensive N-terminal proteomics reveals unknown substrates of the mitochondrial peptidase Icp55. J Proteome Res **12:** 3823–3830

Vidi PA, Kanwischer M, Baginsky S, Austin JR, Csucs G, Dörmann P, Kessler F, Bréhélin C (2006) Tocopherol cyclase (VTE1) localization and vitamin E accumulation in chloroplast plastoglobule lipoprotein particles. J Biol Chem **281:** 11225–11234

Vizcaíno JA, Côté RG, Csordas A, Dianes JA, Fabregat A, Foster JM, Griss J, Alpi E, Birim M, Contell J, et al (2013) The PRoteomics IDEntifications (PRIDE) database and associated tools: status in 2013. Nucleic Acids Res **41:** D1063–D1069

Vögtle FN, Wortelkamp S, Zahedi RP, Becker D, Leidhold C, Gevaert K, Kellermann J, Voos W, Sickmann A, Pfanner N, et al (2009) Global analysis of the mitochondrial N-proteome identifies a processing peptidase critical for protein stability. Cell **139:** 428–439

von Heijne G, Steppuhn J, Herrmann RG (1989) Domain structure of mitochondrial and chloroplast targeting peptides. Eur J Biochem **180:** 535–545

Wessel D, Flügge UI (1984) A method for the quantitative recovery of protein in dilute solution in the presence of detergents and lipids. Anal Biochem **138:** 141–143

Yoo SD, Cho YH, Sheen J (2007) Arabidopsis mesophyll protoplasts: a versatile cell system for transient gene expression analysis. Nat Protoc **2:** 1565–1572

Zybailov B, Rutschow H, Friso G, Rudella A, Emanuelsson O, Sun Q, van Wijk KJ (2008) Sorting signals, N-terminal modifications and abundance of the chloroplast proteome. PLoS ONE **3:** e1994